Master's Thesis of Engineering

Efficient production of (*S*)-limonene and geraniol by peroxisomal compartmentalization of the monoterpene biosynthetic pathway in *Saccharomyces cerevisiae*

Production de (*S*)-limonène et de géraniol par la compartimentalisation de la voie de biosynthèse des monoterpènes dans le peroxysome chez *Saccharomyces cerevisiae*

August 2023

Graduate School of Chemical and Biological Engineering

Seoul National University

Armand Yves Henri Bernard

Efficient production of *(S)*-limonene and geraniol by peroxisomal compartmentalization of the monoterpene biosynthetic pathway in *Saccharomyces cerevisiae*

Examiner: Professor Ji-Sook Hahn

Submitting a master's thesis of

Engineering

May 2023

Graduate School of Chemical and Biological Engineering

Seoul National University

Armand Yves Henri Bernard

Confirming the master's thesis written by

Armand Yves Henri Bernard

June 2023

Chair	황석연 (Seal)
Vice Chair	한지숙 (Seal)
Examiner	조장환 (Seal)

Abstract

Many monoterpenoids have valuable applications in the cosmetics, food, fuel, and pharmaceutical industries (e.g. geraniol, (*S*)-limonene and (*S*)-perillyl alcohol). Due to their versatility, the market demands for monoterpenoids have been growing over the past decades, highlighting the need for an environmentally friendly, stable, and cost-effective synthesis of these molecules. With the rapid development of metabolic engineering tools, microbial hosts have emerged as a promising alternative to produce valuable molecules. The baker's yeast *S. cerevisiae* possesses an efficient endogenous mevalonate (MVA) pathway, produces naturally high amounts of sterols, and is resistant to toxic chemicals and stressful industrial fermentation conditions, making it suitable for large-scale production of monoterpenoids.

In this study, metabolic engineering of the yeast *S. cerevisiae* was carried out to build robust platform strains for geraniol and (*S*)-limonene synthesis. Monoterpenoids are produced from geranyl pyrophosphate (GPP) through the MVA pathway. Erg20 is a farnesyl pyrophosphate synthetase catalyzing two sequential condensations of isopentenyl pyrophosphate (IPP); first, with dimethylallyl pyrophosphate (DMAPP) to produce GPP, and second, with GPP to produce farnesyl pyrophosphate (FPP). As the GPP node is critical in monoterpenoid production, the carbon flux was redirected to the product formation by fusing $Erg20^{WWG}$, a novel mutant with reduced FPP synthesis activity, to a truncated (*S*)-limonene or geraniol synthase lacking their plastid-targeting sequence. Then, peroxisomal compartmentalization of the whole MVA pathway and the $Erg20^{WWG}$-fused monoterpenoid synthases increased the product formation through better precursor utilization. In addition, wild-type *ERG20* was downregulated using the glucose-sensing *HXT1* promoter to redirect the carbon flux of the GPP node towards product formation more efficiently. After further optimizations and multicopy integration of key genes, the final (*S*)-limonene and geraniol platform strains produced 1062.96 mg/L of (*S*)-limonene, the best-achieved titer in a yeast host,

and 1233.54 mg/L of geraniol after a 6-day fed-batch cultivation through glucose and ethanol feeding. These strains reached a gram-scale monoterpenoid titer, making them suitable to produce diverse valuable derivatives of geraniol and *(S)*-limonene.

Keywords: Metabolic engineering, (*S*)-(-)-Limonene, Geraniol, Peroxisome, Erg20, *Saccharomyces cerevisiae*

Student Number: 2022-20248

Content

List of tables

List of figures

Chapter 1. Introduction

Chapter 1. Introduction

1.1. Literature overview

1.1.1 Significance of terpenoids microbial production

Terpenoids, also known as isoprenoids, are the major metabolite family found in nature. Mostly isolated from plants but present in all life kingdoms, they play key roles in all aspects of the cell life cycle, ranging from growth promotion to environmental interactions, as well as cell maintenance [1]. They are compounds of primary and secondary cell metabolism [2]. Even if more than 50,000 terpenoids have been discovered, many of them are yet to be characterized [3]. A broad structural diversity and an even greater variety of activities make these compounds highly valuable for humans. Terpenoids can be used as pharmaceuticals, biofuels, cosmetics, pesticides, and flavoring agents to name a few [4]–[7].

Terpenoids are all derived from the same isoprene (C5) precursors. These monomers are the building blocks for hemi- (1 isoprene unit, C5), mono- (2 units, C10), sesqui- (C15), di- (C20), sester- (C25), tri- (C30), tetra- (C40), and polyterpenes synthesis (more than 8 units, C>40). After this step, functionalization by tailoring enzymes (generally cytochrome P450 enzymes) will give the terpenoids their diverse activities [8]. Two distinct terpenoid biosynthetic pathways exist in nature, with either mevalonate (MVA, e.g. *S. cerevisiae*) or methylerythritol 4-phosphate (MEP, e.g. *E. coli*) as a main intermediate, depending on the organism.

With such a wide range of applications, terpenoids have been indirectly used for centuries [9] because of their high concentration in plants [10]. However, their biological activities were first proven and studied in the 1960s. Promising pharmaceutical applications from the anti-malarian drug artemisinin [5] and other terpenoids have accelerated research and interest, but the chemical synthesis of these complex molecules is energy-consuming, polluting,

and generally results in low yields [11], so not economically viable. That is why terpenoid production from plants has been preferred, but even if this process is greener than chemical synthesis, a large amount of costly and polluting organic solvents is needed to extract and purify the terpenoids from the plant's biomass, and the yields are generally not high enough to meet the growing demand [12]. With the rise of white biotechnology, knowledge, and tools to unveil the potential of microorganisms, an alternative approach to produce terpenoids and their derivatives has been developed, which is designing industrial cell factories using synthetic biology, satisfying economic, environmental, and safety concerns. Success stories such as the high-titer production of antimalarial drug artemisinin (25 g/L) [13] or the production of anti-cancer drug vinblastine by introducing complex biosynthetic pathway (34 heterologous genes in a yeast chassis) [14] highlight the potential of terpenoid microbial production. However, one must bear in mind that despite constant technology development efforts and breakthroughs in cell factories, there are still many challenges to be addressed for the industrial-scale microbial production of a broad range of terpenoids.

1.1.2. Monoterpenoids microbial biosynthesis and research milestones

Monoterpenoids are the smallest terpenoids after hemiterpenoids. They are composed of a monoterpene core ($C_{10}H_{16}$). Due to their unique structure, monoterpenoids are generally more volatile than other terpenoids. They are the main component of plant essential oils, hence widely used in perfumery. In nature, they are responsible for the scent of many plants such as (–)-menthol in mint, geraniol in rose and geranium, or α-pinene in pine trees. They play critical roles in these plants, as they attract pollinators and deter predators [4]. Besides high volatility, monoterpenoids have high calorific values, making them an emerging alternative for fuel applications (e.g. α-pinene and (*R*)/(*S*)-limonene) [15], [16]. In addition, several

monoterpenoids have promising anti-cancer (e.g. geraniol, (*S*)-perillyl alcohol), anti-microbial/fungi (e.g. (*R*)/(*S*)-limonene, 1,8-cineole) or other pharmaceutical activities [17]–[19].

Due to their various applications, the market demand for monoterpenoids has been growing over the past decades, highlighting the need for an environmentally friendly, stable, and cost-effective synthesis of these molecules. As previously said, terpenoid microbial production has gained great interest in the scientific and industrial fields as it offers a lot of advantages over plant biomass extraction. Monoterpenoids are no exception, even if their biosynthesis is plagued with unique challenges [20]. Their volatility and toxicity [21] make them difficult to produce in a heterologous host. The monoterpenoid synthases and cyclases, mostly from plant origin, often exhibit low activity in microbial hosts. Nevertheless, biphasic fermentation [22] and enzyme engineering are common tools to alleviate these challenges. Moreover, the universal precursor of monoterpenoids, geranyl pyrophosphate (GPP), is also utilized to produce steroids or other metabolites in the cell. These competing pathways limit the GPP availability for monoterpenoid synthesis, resulting in low titers compared to the microbial production of other terpenoids [20].

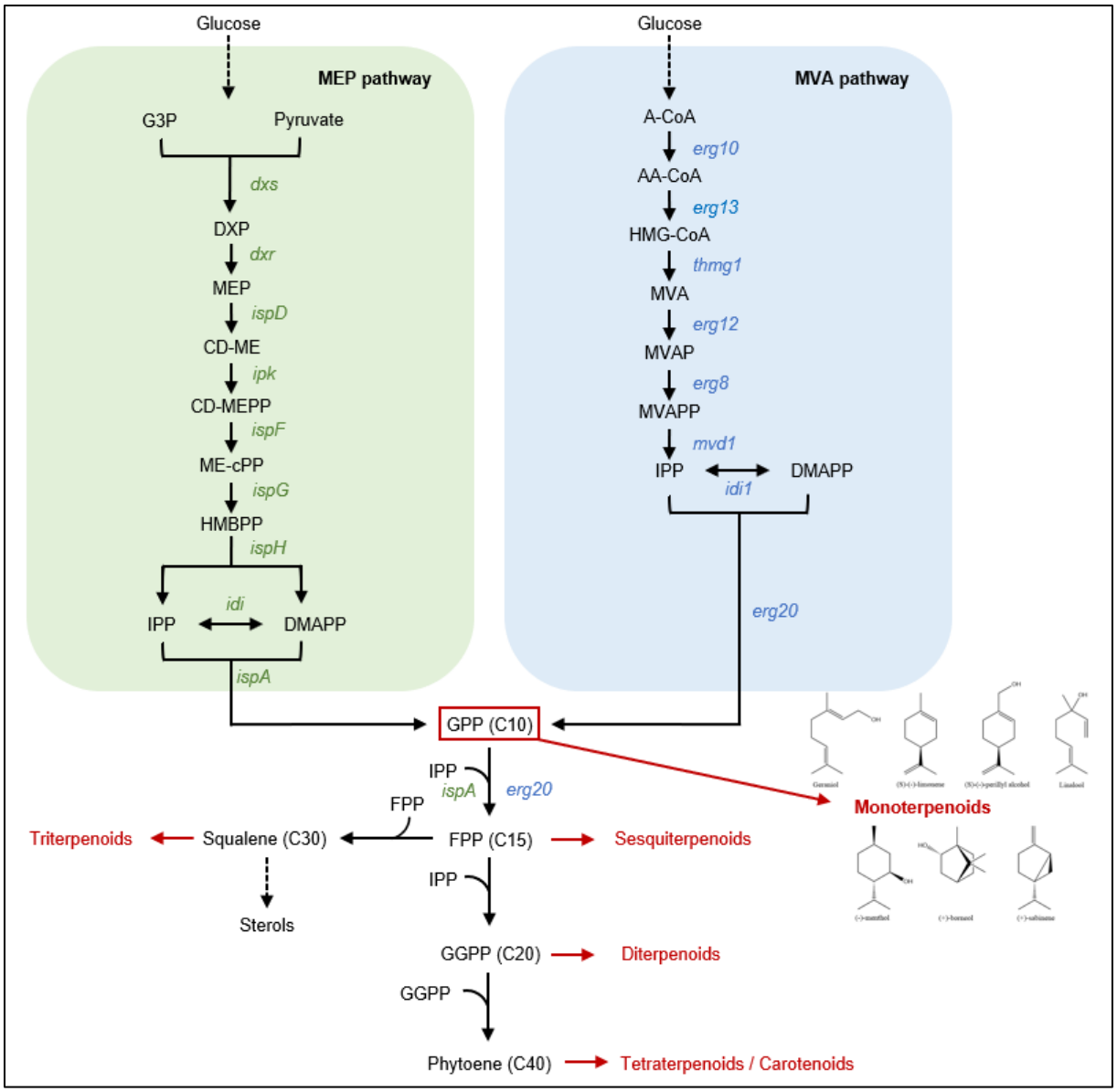

Figure 1: Monoterpenoid biosynthesis pathways.
On the left, the methylerythritol 4-phosphate (MEP) pathway. The genes of *E. coli* involved in the pathway are shown in green. On the right, the mevalonate (MVA) pathway. The genes of *S. cerevisiae* involved in the pathway are shown in blue. The displayed monoterpenoid structures, from left to right, are as follows: geraniol, (*S*)-(-)-limonene, (*S*)-(-)-perillyl alcohol, Linalool, (-)-menthol, (+)-borneol, and (+)-sabinene.

GPP is synthetized from two precursors, isopentenyl pyrophosphates (IPP) and its isomer, dimethylallyl pyrophosphate (DMAPP) (Fig. 1), in both the MVA and the MEP pathways. The main reason for the low native GPP availability is due to the enzyme catalyzing GPP synthesis (IspA in the MEP pathway and Erg20 in the MVA pathway). This enzyme also utilizes GPP as a substrate to produce farnesyl diphosphate (FPP), a precursor of the other

terpenoids and sterols. To overcome this challenge, several mutants of IspA [23] and Erg20 [24], [25] with altered substrate specificity were engineered in *E. coli* and *S. cerevisiae* (the preferred microbial hosts for monoterpenoid production).

Since then, several milestones have been reached in the last two decades, mainly driven by advancements in our understanding of cell metabolism and the mass discovery of monoterpenoid synthase candidates through novel bioinformatic tools, legitimizing the cell factories for the synthesis of a wide range of valuable monoterpenoids. Even if *E. coli* or other bacterial hosts have undeniable advantages for the production of valuable molecules, yeast chassis have been preferred for monoterpenoids biosynthesis in the last years [26], especially *S. cerevisiae*. In the next section, the advantages of choosing *S. cerevisiae* as a platform stain for monoterpenoid production will be discussed, as well as some of the major breakthroughs in this field.

1.1.3. *S. cerevisiae* as a monoterpenoid biosynthesis platform

The baker's yeast S. *cerevisiae* has been preferred over other microorganisms to produce various compounds [27]. Monoterpenoid production is no exception, as this yeast possesses several advantages over the other common candidates such as *E. coli*. Besides being a well-known, stable, and safe organism (so inherently having a large number of genetic engineering tools at disposal) [26], [28], *S. cerevisiae* has unique traits that are especially valuable for monoterpenoid synthesis. The baker's yeast possesses an efficient endogenous MVA pathway and produces naturally higher amounts of sterols than other candidates. For instance, a common monoterpenoid production engineering strategy in *E. coli* is the introduction of the whole MVA pathway of *S. cerevisiae* in the cell [23]. The yeast's resistance to stressful industrial fermentation conditions (low pH, high cell density and sugar titer, etc.) makes it suitable for large-scale monoterpenoid production. Its robustness is essential as most of the monoterpenoids

and their precursors have significant cytotoxicity [21]. As an eukaryotic cell, *S. cerevisiae* is known for the efficient expression of membrane-bound cytochrome P450 enzymes (CYP) thanks to their posttranslational modification processes [29]. Since most of the monoterpenes tailoring enzymes are CYPs, the production of monoterpenoids and their derivatives will be more straightforward in a *S. cerevisiae* chassis (several *S. cerevisiae* strains were specifically engineered to accept CYPs from higher eukaryotes with ease). However, the monoterpenoid synthases candidates still have to be selected carefully, as activity in heterologous hosts may vary [29], and good paring of CYPs to a proper reductase (CPR) is critical. Over the years, monoterpenoid production in *S. cerevisiae* hosts went from a microgram-scale to industrially and economically viable gram-scale titers due to many breakthroughs (see Table 1).

Table 1: Noteworthy engineering strategies in *S. cerevisiae* monoterpenoid production

Host	Monoterpenoid	Main engineering strategy	Scale	Titer	Ref.
S. cerevisiae Y21258	Geraniol	GPPS mutant *ERG20** (K197G)	Batch	5 mg/L	[23]
S. cerevisiae AM78	Sabinene	GPPS mutant *ERG20** (F96W, N127W), stabilized *HMG2** mutant (K6R), monoallelic *ERG9Δ* (downregulation), GPPS and monoterpenoid synthase fusion	Batch	17.5 mg/L	[24]
S. cerevisiae CEN.PK2-1C	Geraniol	Truncated *HMG1*, *IDI1*, *MAF1* and *ERG20** (K197G) overexpression	Batch	36.04 mg/L	[30]
S. cerevisiae CEN.PK102-5B	Geraniol	Mutated transcription factor *UPC2** (G888D), *ERG20** (F96W, N127W), *IDI1* and *tHMG1* overexpression, GPPS and monoterpenoid synthase fusion	Fed-batch	293 mg/L	[31]
S. cerevisiae CEN.PK102-5B	Geraniol	Native *ERG20* downregulation with *HXT1* promoter, *OYE2Δ*, *ERG20** (F96W, N127W), *UPC2** (G888D), *IDI1* and *tHMG1* overexpression, *BTS1* downregulation,	Fed-batch	650.8 mg/L	[32]
S. cerevisiae CEN.PK2-1C	Linalool and (*R*)-limonene	Native *ERG20* downregulation by N-degron destabilization, *ERG20** (F96W, N127W), *HMG2** (K6R), *EfmvaS* and *EfmvaE* from *E. faecalis*, *MVD1* and *IDI1* overexpression	Batch	18 and 76 mg/L	[33]
S. cerevisiae CEN.PK2-1C	(*R*)-limonene	Orthogonal biosynthetic pathway: *SlNdps1* heterologous overexpression from *S.*	Fed-batch	917.7 mg/L	[34]

		lycopersicum catalyzing neryl diphosphate (NPP, cis-GPP) formation from IPP and DMAPP instead of GPP, *ERG20** (F96W, N127W), *tHMG1* and *IDI1* overexpression, native *ERG20* downregulation with *HXT1* promoter			
S. cerevisiae EGY48	(*R*) and (*S*)-limonene, geraniol, 8-hydroxygeraniol, sabinene, camphene, α-pinene, *trans*-isopiperitenol	Peroxisomal compartmentalization of the whole MVA pathway (*ERG20** (F96W, N127W), *EfmvaS* and *EfmvaE* from *E. faecalis* overexpression)	Batch and Fed-batch (30 days, for geraniol and *(R)*-limonene)	Batch: 141.46, 51.98, 288.65, 25.11, 32.32, 5.77, 69.22 and 19.24 mg/L Fed-batch: 5.52 and 2.58 g/L	[35]

As previously mentioned, the GPP node in the MVA pathway is critical for monoterpenoid synthesis. GPP is synthesized and produced by the same enzyme, Erg20 (Fig. 1), so its accumulation remained a challenge for a long time. As a basal FPP synthesis from GPP is essential for yeast growth, deleting native *ERG20* and replacing it with a heterologous strict GPP synthase was not a solution. Over the years several *ERG20* mutants with an altered substrate specificity (favoring GPP synthesis over FPP) were discovered [24], with a double mutant being the most suitable candidate [25]. Their usage for geraniol or sabinene production in *S. cerevisiae* helped to break the µg/L barrier and reach mg/L scale. Shortly after, several rate-limiting enzymes in the MVA pathway were identified, such as Hmg1 (and/or Hmg2) and Idi1 (as the native DMAPP/IPP ratio is suboptimal for product synthesis). The truncation of *HMG1* to remove its membrane-binding domain [30], the mutation of *HMG2* to improve its

stability [24] and the global overexpression of several or all of the MVA pathway genes increased monoterpenoids titers even more. Also, the mutated transcription factor Upc2-1 (G888D) was shown to upregulate the MVA and the sterol synthesis pathways as a whole [31]. Generally, improving the carbon flux in the MVA pathway not only benefited monoterpenoid production but also other terpenoids.

Another noticeable engineering strategy for monoterpenoid biosynthesis is the fusion of the heterologous monoterpenoid synthase to the mutated GPP synthase *ERG20** [31]. This helped to drag the carbon flux towards product synthesis even more, by improving the substrate availability for the monoterpenoid synthase, known to exhibit low catalytic activities, and became a common strategy. However, gene fusion must be assessed case by case, as monoterpenoid synthases' structures have a large variability. The linker choice must also be considered [36].

Overexpressing a mutated copy of *ERG20* may not be sufficient, as the native *ERG20* gene is still expressed in the yeast's genome. To reduce the carbon flux towards FPP synthesis even more, several strategies were tested to find the optimal way to downregulate the native *ERG20*. Leaky promoters such as P_{MET3}, the copper-repressible promoter P_{CTR3}, or the weak P_{BTS1} were tested without noticeable improvement of monoterpenoid titer [32]. The sterol-responsive promoter P_{ERG1} coupled to Erg20 destabilization with the N-degron rule leads to titer improvement [33], but the best downregulation so far is by using a glucose-sensing promoter such as P_{HXT1} [32] or P_{HXT3} [14], [37]. In this case, when glucose is present in the culture medium, the promoter upregulates *ERG20*, leading to enhanced sterol synthesis and growth. When glucose is depleted or lacking (more likely after the diauxic shift), $P_{HXT1/3}$ represses *ERG20*, and most of the carbon flux in the MVA pathway will be diverted to product synthesis. This strategy is particularly efficient when coupled to an ethanol-fed-batch strategy [34], as the

majority of the carbon source will be used for product synthesis after glucose depletion [38]. This type of downregulation may also be used for the production of other terpenoids (e.g. *ERG9* downregulation for carotenoid production [39]).

Another way to deal with the challenges of the GPP node was recently found [34]. Instead of using GPP as a substrate for (*R*)-limonene synthesis, neryl diphosphate (NPP, cis-GPP) was produced from DMAPP and IPP with an NPP synthetase from *S. lycopersicum*. The produced NPP cannot be used by Erg20 to make FPP, so all of it will be used for (*R*)-limonene formation. This novel method has been tried for other monoterpenoids with great success, but one must bear in mind that not all monoterpenoid synthases can accept NPP as a substrate as well as GPP, and can result in byproduct formation [20].

As several MVA pathway intermediates are also consumed in competing pathways, its isolation may be an efficient strategy to avoid unnecessary leakage. Compartmentalizing the monoterpenoid pathway into the yeast peroxisomes led to a dramatic fold increase for several monoterpenoid synthases [35]. In addition to isolation from competing pathways, peroxisomes offer several advantages. The β-oxidation of fatty acids inside the peroxisome creates a significant acetyl-CoA pool that can be used in the MVA pathway, as 3 molecules of acetyl-CoA are necessary for the formation of 1 molecule of GPP. Peroxisomal compartmentalization can also help the cell to handle greater titers of monoterpenoids, as peroxisomes naturally act as detoxifying agents in the cell.

After building a proper strain for monoterpenoid biosynthesis, choosing the right fermentation conditions is crucial. Regarding product cytotoxicity, the use of organic solvents in a biphasic fermentation drastically reduces the impact on cell growth [22]. As monoterpenoids are volatile, trapping them in an organic layer greatly reduces evaporation loss. Several solvents can be used in that regard, but their toxicity toward cells must be considered.

Isopropyl myristate (IPM) may be a suitable candidate and has been widely used recently. It is important to mention that this biphasic fermentation strategy is efficient to extract monoterpenoids directly synthetized from GPP, but could be a problem for the synthesis of derivatives. For instance, the synthesis of (*S*)-perillyl alcohol from (*S*)-limonene in a biphasic culture might be impeded due to early (*S*)-limonene extraction to the organic phase before its conversion to (*S*)-perillyl alcohol [40].

Batch cultures are used to assess strains' capabilities, but fed-batch or continuous cultures are the preferred choices for industrial-scale productions. Several parameters must be monitored in this matter, such as pH, aeration, and medium type. The carbon source for the initial culture and the feeding are critical not only for monoterpenoid production but in all bioprocesses. Since monoterpenoids are secondary metabolites, their synthesis is favored under partial or total ethanol consumption [41].

Monoterpenoid biosynthesis in *S. cerevisiae* also transitioned from the microgram- scale to gram-scale production with the help of powerful bioinformatic tools. The process of genome mining helped to discover a broad range of monoterpenoid synthase candidates. Thanks to protein folding and 3D-structure resolution, our understanding of their mode of action increased a lot. Hence, enzyme engineering to obtain mutants with better stability, catalytic power, etc. was greatly simplified.

However, several challenges remain in monoterpenoid and terpenoid microbial production in general. The involved pathways are very demanding in cofactor supply such as NADPH, ATP, or acetyl-CoA. Some efforts were recently made to engineer the PDH bypass [34] for an enhanced acetyl-CoA pool or the use of other enzymes in the MVA pathway that use NADH instead of NADPH [42]. Also, since titers are breaking the gram-scale barrier, the toxicity of monoterpenoids must be considered. Adaptative laboratory evolution might help in

that matter. Even if this method is costly and time-consuming, promising results in monoterpenoid yeast tolerance [43] might help us to understand the metabolic processes involved in this tolerance.

One solution might be to use cell-free systems. They are difficult to set up since sufficient knowledge of the enzymes involved is necessary and efficient production methods are needed, but the toxicity issue is no longer relevant, as well as other cell factories-related challenges. Promising results in this field are already appearing, with great yields and titers [44].

1.2. Research project objectives: (*S*)-limonene, (*S*)-perillyl alcohol, and geraniol as candidates for bioproduction in *S. cerevisiae*

Regarding monoterpenoid synthesis in *S. cerevisiae*, the rapid development of successful metabolic engineering strategies happened in recent years but there is still room for improvement, especially for some types of monoterpenoids. Geraniol has been the most extensively researched one, as the molecule and its derivatives have many uses, mainly in the pharmaceuticals and cosmetics industries. Also, as its synthase shows a high catalytic efficiency compared to other ones [35], geraniol is a suitable candidate to indirectly assess metabolic strategies and genome editing made on the yeast cell. Limonene is also a popular monoterpenoid in microbial production, especially the (*R*) enantiomer. The two enantiomers have similar applications in several fields (pharmaceutical, cosmetics, household, and food applications, etc.), but have distinct smells and are present at different ratios in plants [45]. The (*R*) form is believed to have a citrusy pleasant smell, as the (*S*) form has a more pungent and piney one. Also, choosing which enantiomer to produce is important as their derivatives have different activities. For instance, the limonene derivative perillyl alcohol (POH) naturally occurs in the (*S*) form and is a promising anti-cancer agent currently under several clinical trials

[46]. The potential biological activities of the (*R*) form remain unknown, as only the (*S*) form is under inspection [47]. Also, an enantiomeric purity is usually preferred for therapeutic uses.

In *S. cerevisiae*, (*R*)-limonene synthesis has been preferred mainly due to the lack of suitable GPP cyclase candidates for (*S*)-limonene [16]. There is therefore room for improvement (*S*)-limonene synthesis in *S. cerevisiae* chassis.

(*S*)-POH has been successfully produced in *E. coli* in several studies over the last decade using bacterial CYPs [40] but no quantified amount has been synthetized in *S. cerevisiae*. Recently, a novel (*S*)-POH synthase of plant origin has been discovered [48] and expressed in *S. cerevisiae*, but without a proper cytochrome NADPH-dependent reductase (CPR) and only as a proof of concept.

One of the purposes of this study is to make a robust *S. cerevisiae* (*S*)-limonene platform strain that can produce an adequate amount of monoterpenoid. The (*S*)-limonene titer needs to be sufficiently high for derivatives synthesis. After optimizations, this platform strain will be used to produce the valuable (*S*)-POH using a recently discovered (*S*)-POH synthase. Several metabolic engineering strategies for monoterpenoid production will be tested and assessed by geraniol synthesis and then applied for (*S*)-limonene and (*S*)-POH production. The geraniol platform strain may also be used to produce valuable derivatives in the future.

Chapter 2. Materials and methods

Chapter 2. Materials and methods

2.1. Strains, chemicals, and media

All *S. cerevisiae* strains used in this study are listed in Table 2 and were derived from *S. cerevisiae* CEN.PK2-1C (*MATa URA3-52 TPR1-289 LEU2-3,112 HIS3Δ1 MAL2-8C SUC2*), commonly used for metabolic engineering. The parental strain was purchased from EUROSCARF.

All genetic manipulation and cloning were done using chemically competent *E. coli* DH5α cells (F^- *ϕ80lacZΔM15 Δ(lacZYA-argF)U169 recA1 endA1 hsdR17(*r_K^-, m_K^+*) phoA supE44* λ^-*thi-1 gyrA96 relA1*). Luria-Bertani (LB, tryptone 10 g/L, yeast extract 5 g/L, NaCl 10 g/L) medium supplemented with 50 μg/mL of ampicillin as selection pressure was used for cell culture.

Yeast cells were cultured in YPD rich medium (yeast extract 10 g/L, peptone 20 g/L, glucose 20g/L or more) or in synthetic complete (SC, yeast nitrogen base without amino acids 6.7 g/L, 1.4 g/L amino acids dropout mixture suitable for plasmid selection, and glucose 20 g/L or more) minimal medium. Bacto™ yeast extract, peptone, tryptone, Difco™ dextrose and agar were purchased from BD Bioscience (Franklin Lakes, NJ, USA). Yeast nitrogen base (YNB), amino acids for dropout mixture, and HPLC standard materials were all purchased from Sigma-Aldrich (St. Louis, MO, USA).

Table 2: Strains used in this study

Strain name	Description	Genotype	Reference
E. coli DH5α	Strain used for cloning	F^- ϕ80lacZΔM15 Δ(lacZYA-argF)U169 recA1 endA1 hsdR17(r_K^-, m_K^+) phoA supE44 λ^-thi-1 gyrA96 relA1	
S. cerevisiae CEN.PK2-1C	Wild type parental strain	MATa *URA*3-52 *TRP*1-289 leu2-3,112 *HIS*3Δ1 MAL2-8^C SUC2	EUROSCARF, [49]
JHY01	GPP accumulation strain	CEN.PK2-1C; H4::P_{TEF1}-*tHMG1*-T_{ADH1}-P_{TDH3}-*ERG20*^{WWG}-T_{TPS1}	This study
JHY02	GPP accumulation with *ERG*20 N-Degron downregulation	JHY01 derivative; *ERG20*(-304, 3):: P_{ERG1}-*UBI4*-Degron(F:K3K15)	This study, [33]
JHY03	GPP accumulation with *ERG20* P_{HXT1} downregulation	JHY01 derivative; *ERG20*(-304, -1)::P_{HXT1}	This study
JHY04	Delta-integration of *ERG20*^{WWG} and *tHMG1* with the *TRP1* marker	CEN.PK2-1C; δ::loxP-*TRP1*-loxP-P_{TDH3}-*ERG20*^{WWG}-T_{TPS1}-P_{TEF1}-*tHMG1*-T_{ADH1}	This study
JHYG01	Geraniol production by *tCrGES* overexpression (OE) on plasmid	CEN.PK2-1C harboring Coex413-*tCrGES* plasmid	This study
JHYG02-1	Control for Geraniol production using *ERG20* mutants	CEN.PK2-1C harboring Coex413-*tCrGES* and Coex415-*ERG20*	This study
JHYG02-2	*tCrGES* and *ERG20*^{G} OE on plasmid	CEN.PK2-1C harboring Coex413-*tCrGES* and Coex415-*ERG20*^{G}	This study
JHYG02-3	*tCrGES* and *ERG20*^{W} OE on plasmid	CEN.PK2-1C harboring Coex413-*tCrGES* and Coex415-*ERG20*^{W}	This study
JHYG02-4	*tCrGES* and *ERG20*^{WW} OE on plasmid	CEN.PK2-1C harboring Coex413-*tCrGES* and Coex415-*ERG20*^{WW}	This study
JHYG02-5	*tCrGES* and *ERG20*^{WWG} OE on plasmid	CEN.PK2-1C harboring Coex413-*tCrGES* and Coex415-*ERG20*^{WWG}	This study
JHYG03	*tCrGES*, *ERG20*^{WWG} and *tHMG1* OE on plasmid	CEN.PK2-1C harboring Coex413-*tCrGES* and Coex415-*tHMG1*,*ERG20*^{WWG}	This study
JHYG04-1	Control for Geraniol production by fusion proteins	JHY01 harboring Coex413-*tCrGES* and Coex415-*ERG20*^{WWG}	This study
JHYG04-2	*ERG20*^{WWG}-G_6-*tCrGES* OE on plasmid in JHY01	JHY01 harboring Coex413-*ERG20*^{WWG}-G_6-*tCrGES*	This study
JHYG04-3	*tCrGES*-G_6-*ERG20*^{WWG} OE on plasmid in JHY01	JHY01 harboring Coex413-*tCrGES*-G_6-*ERG20*^{WWG}	This study

JHYG05	MVA pathway peroxisomal targeting for Geraniol on plasmid	CEN.PK2-1C harboring Coex413-*MVD1*-ePTS1,*ERG10*-ePTS1,*tCrGES*-G_6-*ERG20*^{WWG}-ePTS1, Coex415-*tHMG1*-ePTS1,*ERG13*-ePTS1,*ERG8*-ePTS1 and Coex416-*ERG12*-ePTS1,*IDI*1-ePTS1,*ERG20*^{WWG}-ePTS1	This study
JHYG06	Geraniol Peroxisomal production strain	CEN.PK2-1C; H1::P_{PGK1}-*MVD1*-ePTS1-T_{PGK1}-P_{TPI1}-*ERG10*-ePTS1-T_{TPI1}-P_{TDH3}-*tCrGES*-*G*$_6$-*ERG20*^{WWG}-ePTS1-T_{TPS1} H5::P_{TDH3}-*tHMG1*-ePTS1-T_{GPM1}-P_{TEF1}-*ERG13*-ePTS1-T_{ADH1}- P_{TPI1}-*ERG8*-ePTS1-T_{TPI1} H7::P_{PGK1}-*ERG12*-ePTS1-T_{PGK1}-P_{TEF1}-*IDI1*-ePTS1-T_{ADH1}-P_{TDH3}-*ERG20*^{WWG}-ePTS1-T_{TPS1}	This study
JHYG07	Geraniol peroxisomal production and *ERG20* downregulation **(Final Geraniol production strain)**	JHYG06 derivative; *ERG20*(-304, -1)::P_{HXT1}	This study
JHYG08	+ 1 additional copy of *tCrGES*-*G*$_6$-*ERG20*^{WWG} in cytosol	JHYG07 derivative; H8::P_{TDH3}-*tCrGES*-*G*$_6$-*ERG20*^{WWG}-T_{TPS1}	This study
JHYG09	+ 1 additional copy of *tHMG1* and *ERG20*^{WWG} in cytosol	JHYG08 derivative; H4::P_{TEF1}-*tHMG1*-T_{ADH1}-P_{TDH3}-*ERG20*^{WWG}-T_{TPS1}	This study
JHYL01-1	(*S*)-Limonene production by *MsLS* OE on plasmid	JHY01 harboring Coex413-*MsLS*	This study
JHYL01-2	*tMsLS* OE on plasmid	JHY01 harboring Coex413-*tMsLS*	This study
JHYL02-1	Control for (*S*)-Limonene production by fusion proteins	JHY01 harboring Coex413-*tMsLS* and Coex415-*ERG20*^{WWG}	This study
JHYL02-2	*ERG20*^{WWG}-*G*$_6$-*tMsLS* OE on plasmid in JHY01	JHY01 harboring Coex413-*ERG20*^{WWG}-*G*$_6$-*tMsLS*	This study
JHYL02-3	Delta-integration of *ERG20*^{WWG}-*G*$_6$-*tMsLS* with the *TRP1* marker	CEN.PK2-1C; δ::loxP-*TRP1*-loxP-P_{TDH3}-*ERG20*^{WWG}-*G*$_6$-*tMsLS*-T_{TPS1}	This study
JHYL02-4	Delta-integration of *ERG20*^{WWG}-*G*$_6$-*tMsLS* with the *KAN*^{R} marker	CEN.PK2-1C; δ::loxP-*KAN*^{R}-loxP-P_{TDH3}-*ERG20*^{WWG}-*G*$_6$-*tMsLS*-T_{TPS1}	This study
JHYL02-5	*tMsLS*-*G*$_6$-*ERG20*^{WWG} OE on plasmid in JHY01	JHY01 harboring Coex413-*tMsLS*-*G*$_6$-*ERG20*^{WWG}	This study
JHYL03-1	MVA pathway peroxisomal targeting for (*S*)-Limonene on plasmid	CEN.PK2-1C harboring Coex413-*MVD1*-ePTS1,*ERG10*-ePTS1,*ERG20*^{WWG}-*G*$_6$-*tMsLS*-ePTS1, Coex415-*tHMG1*-ePTS1,*ERG13*-ePTS1,*ERG8*-ePTS1 and Coex416-*ERG12*-ePTS1,*IDI1*-ePTS1,*ERG20*^{WWG}-ePTS1	This study

JHYL03-2	MVA pathway peroxisomal targeting for (*S*)-Limonene in JHY02 on plasmid	JHY02 harboring Coex413-*MVD1*-ePTS1,*ERG10*-ePTS1,*ERG20*^{WWG}-*G*$_6$-*tMsLS*-ePTS1, Coex415-*tHMG1*-ePTS1,*ERG13*-ePTS1,*ERG8*-ePTS1 and Coex416-*ERG12*-ePTS1,*IDI1*-ePTS1,*ERG20*^{WWG}-ePTS1	This study
JHYL03-3	MVA pathway peroxisomal targeting for (*S*)-Limonene in JHY03 on plasmid	JHY03 harboring Coex413-*MVD1*-ePTS1,*ERG10*-ePTS1,*ERG20*^{WWG}-*G*$_6$-*tMsLS*-ePTS1, Coex415-*tHMG1*-ePTS1,*ERG13*-ePTS1,*ERG8*-ePTS1 and Coex416-*ERG12*-ePTS1,*IDI1*-ePTS1,*ERG20*^{WWG}-ePTS1	This study
JHYL03-4	MVA pathway peroxisomal targeting for (*S*)-Limonene in *CIT2*Δ strain	CEN.PK2-1C; *CIT2*Δ harboring Coex413-*MVD1*-ePTS1,*ERG10*-ePTS1,*ERG20*^{WWG}-*G*$_6$-*tMsLS*-ePTS1, Coex415-*tHMG1*-ePTS1,*ERG13*-ePTS1,*ERG8*-ePTS1 and Coex416-*ERG12*-ePTS1,*IDI1*-ePTS1,*ERG2*^{WWG}-ePTS1	This study
JHYL04	(*S*)-Limonene Peroxisomal production strain	CEN.PK2-1C; H1::P$_{PGK1}$-*MVD1*-ePTS1-T$_{PGK1}$-P$_{TPI1}$-*ERG10*-ePTS1-T$_{TPI1}$-P$_{TDH3}$-*ERG20*^{WWG}-*G*$_6$-*tMsLS*-ePTS1-T$_{TPS1}$ H5::P$_{TDH3}$-*tHMG1*-ePTS1-T$_{GPM1}$-P$_{TEF1}$-*ERG13*-ePTS1-T$_{ADH1}$- P$_{TPI1}$-*ERG8*-ePTS1-T$_{TPI1}$ H7::P$_{PGK1}$-*ERG12*-ePTS1-T$_{PGK1}$-P$_{TEF1}$-*IDI1*-ePTS1-T$_{ADH1}$-P$_{TDH3}$-*ERG20*^{WWG}-ePTS1-T$_{TPS1}$	This study
JHYL05	(*S*)-Limonene Peroxisomal production strain and *ERG20* downregulation	JHYL04 derivative; *ERG20*(-304, -1)::P$_{HXT1}$	This study
JHYL06	+ 1 additional copy of *ERG20*^{WWG}-*G*$_6$-*tMsLS* in cytosol	JHYL05 derivative; H8::P$_{TDH3}$-*ERG20*^{WWG}-*G*$_6$-*tMsLS*-T$_{TPS1}$	This study
JHYL07	+ 2 additional copies of *ERG20*^{WWG}-*G*$_6$-*tMsLS* in cytosol **(Final (*S*)-Limonene production strain)**	JHYL06 derivative; H2::P$_{TDH3}$-*ERG20*^{WWG}-*G*$_6$-*tMsLS*-T$_{TPS1}$	This study
JHYL08	+ 3 additional copies of *ERG20*^{WWG}-*G*$_6$-*tMsLS* in cytosol	JHYL07 derivative; H4::P$_{TDH3}$-*ERG20*^{WWG}-*G*$_6$-*tMsLS*-T$_{TPS1}$	This study
JHYL09	(*S*)-Limonene peroxisomal production, 2 additional copies of *ERG20*^{WWG}-*G*$_6$-*tMsLS* and 1 additional copy of *tHMG1* and *ERG20*^{WWG} in cytosol	JHYL07 derivative; H4::P$_{TEF1}$-*tHMG1*-T$_{ADH1}$-P$_{TDH3}$-*ERG20*^{WWG}-T$_{TPS1}$	This study
JHYP01-1	(*S*)-Perillyl alcohol control strain	JHYL04 harboring Coex413-*SdL7H* and Coex415-ev plasmids	This study

JHYP01-2	*SdL7H* and *NCP1* OE	JHYL04 harboring Coex413-*SdL7H* and Coex415-*NCP1* plasmids	This study
JHYP01-3	*SdL7H* and *PfCPR* OE	JHYL04 harboring Coex413-*SdL7H* and Coex415-*PfCPR* plasmids	This study
JHYP02	(*S*)-Perillyl alcohol production strain	JHYL04 derivative; H4::P_{TDH3}-*SdL7H*-T_{TPS1}-P_{PGK1}-*PfCPR*-T_{PGK1}	This study
JHYP03	*INO2* OE on plasmid	JHYP02 harboring Coex415-*INO2* plasmid	This study
JHYP04	*ICE2* OE on plasmid	JHYP02 harboring Coex415-*ICE2* plasmid	This study
JHYP05	(*S*)-Perillyl alcohol production strain *PAH1*Δ	JHYP02 derivative; *PAH1*Δ	This study
JHYP06-1	(*S*)-Perillyl alcohol production with *SdL7H* and *PfCPR* fusion	JHYL04 harboring Coex413-*SdL7H-*G_6*-46tPfCPR* plasmid	This study
JHYP06-2	(*S*)-Perillyl alcohol production with *PfCPR* and *SdL7H* fusion	JHYL04 harboring Coex413-*PfCPR-*G_6*-18tSdL7H* plasmid	This study
JHYP06-3	(*S*)-Perillyl alcohol production with *SdL7H* and *tMsLS* fusion and *PfCPR* OE	JHYL04 harboring Coex413-*SdL7H-*G_6*-tMsLS* and Coex415-*PfCPR* plasmids	This study
JHYP06-4	(*S*)-Perillyl alcohol production with *SdL7H* and *ERG20*^{WWG}-G_6-*tMsLS* fusion and *PfCPR* OE	JHYL04 harboring Coex413-*SdL7H-*G_6*-ERG20*^{WWG}-G_6-*tMsLS* and Coex415-*PfCPR* plasmids	This study
JHYP07	(*S*)-Perillyl alcohol production by high copy *SdL7H* and *PfCPR* OE on plasmids	JHYL04 harboring Coex423-*SdL7H,PfCPR* plasmid	This study

2.2. Construction of plasmids and strains

The plasmids used in this study are listed in Table 3. Plasmid construction and manipulation were done by restriction-ligation cloning. All restriction enzymes, T4 ligase, and cloning reagents were purchased from Thermo Fisher Scientific (Waltham, MA, USA). Prior to transformation in *E. coli* DH5α competent cells, genetic parts were PCR-amplified using BioFACT™ lamp pfu or pfu DNA polymerases (Biofact, Muar, Johor, Malaysia) with primers flanked by restriction sites (listed in Table 4), restricted and ligated. Except integration vectors, all plasmids were shuttle plasmids, harboring both *E. coli* and *S. cerevisiae* genetic features

(*amp*^{R} gene and ori replication origin for *E. coli* and proper *HIS3*, *TRP1*, *LEU2* or *URA3* gene and CEN/ARS replication origin for low copy or 2μ for high copy for *S. cerevisiae*). Multigene-expression vectors (Coex) were used as previously described [50].

S. cerevisiae CEN.PK2-1C genomic DNA used for PCR was extracted using the PCI method [51] for further cassette construction or the lithium acetate-SDS buffer method [52] for yeast genotypes verifications. All primers were synthetized by BIONICS (Seoul, Korea). Genome-edited strains were verified through sequencing by Celemics (Seoul, Korea). Plasmid extraction, PCR purification and gel extraction LaboPass™ kits were purchased from Cosmo Genetech (Seoul, Korea). A Lithium-Acetate/Salmon Sperm DNA/PEG method [53] with DMSO treatment was used for yeast transformation.

Yeast genome-editing was mainly performed using a CRISPR/Cas9 system as previously described [54]. Proper guide RNA sequence were found using the CHOPCHOP DNA tool from the University of Bergen [55]. For gene deletion, a donor DNA fragment consisting of 50 base pairs upstream and downstream of the ORF was PCR-amplified and transformed into the cell. For promoter replacement, the new promoter was amplified with primers flanked by 35-bp downstream and upstream of the targeted region. For cassette integration, sites nearby highly expressed genes were chosen based on previous research [56]. H1, H2, H4, H5, H7 and H8 sites were utilized for cassettes integration. Since several cassettes (up to 3) were integrated into the same site, a 500-bp homology region was chosen for an increased homologous recombination (HR) efficiency. Cas9 and gRNA components were expressed on two different plasmids and transformed into the cell with the proper donor DNA fragment. For cassette integration, promoters, ORFs, and terminators were sequentially cloned into a Coex integration vector (no yeast replication origin). H sites were flanked by SmiI sites to ensure plasmid digestion before transformation with the correct plasmids. After

CRISPR/Cas9 genome-editing, Cas9 and guide RNA plasmids were removed through YPD cultures before making the cell stock.

For multi-copy cassette integration trials, a delta-integration method was used as previously described [57]. There are hundreds of retrotransposon Ty1 long terminal repeats (LTR) sequences in the genome of *S. cerevisiae*, which are known as delta-sequences [58]. Those δ-sites are a popular target for copy number fine-tuning of overexpressed cassettes [59]. In this study, integration was performed by HR using the tryptophan (*TRP1*) marker and the Cre-loxP recombination system [60] was used to recover this auxotrophic marker gene. Delta-integration using the CRISPR/cas9 system was also tried.

Table 3: Plasmids used in this study

Plasmid name	**Relevant characteristics**
Coex413/4/5/6-X	Multigene-expression vector (Coex) shuttle vector with *E. coli* (*amp*^{R} marker and ori replication origin) and *S. cerevisiae* features (CEN/ARS replication origin (low copy) and *HIS3*, *TRP1*, *LEU2* or *URA3* marker gene)
Coex413/4/5/6-ev	Coex plasmid without ORF (empty vector for control) harboring strong promoter and terminator
pRS413-Ndegron	CEN/ARS *HIS3* vector harboring N-degron cassette (P$_{ERG1}$-*UBI4*-FK3K15) [33]
pRS-delta-loxP-TRP-loxP-*tHMG1,ERG20*^{WWG}	pRS vector harboring *trp1* marker gene flanked by loxP sequences as well as P$_{TEF1}$-*tHMG1*-T$_{ADH1}$ and P$_{TDH3}$-*ERG20*^{WWG}-T$_{TPS1}$ cassettes. 170-bp homology arms upstream and downstream the delta sequences are flanking the 3 cassettes. Donor DNA can be extracted from the vector by SmiI digestion
pRS-delta-loxP-TRP-loxP-*ERG20*^{WWG}-*G$_6$-tMsLS*	Same features as pRS-delta-loxP-TRP-loxP-*tHMG1,ERG20*^{WWG}, except the cassette for delta-integration, which is P$_{TDH3}$-*ERG20*^{WWG}-*G$_6$-tMsLS*-T$_{TPS1}$
pRS-delta-loxP-KanMX-loxP-*ERG20*^{WWG}-*G$_6$-tMsLS*	Same features as pRS-delta-loxP-TRP-loxP-*ERG20*^{WWG}-*G$_6$-tMsLS*, but the marker gene in *KAN*^{R}
Coex415-*ERG20*	Coex plasmid harboring P$_{TDH3}$-*ERG20*-T$_{TPS1}$ cassette
Coex415-*ERG20*^{W}	Generated by DpnI mutagenesis of Coex415-*ERG20*
Coex415-*ERG20*^{WW}	
Coex415-*ERG20*^{G}	
Coex415-*ERG20*^{WWG}	
Coex415-*UPC2*	Coex plasmid harboring P$_{TEF1}$-*UPC2*-T$_{ADH1}$ cassette
Coex415-*UPC2*^{G888D}	Generated by DpnI mutagenesis or Coex415-*UPC2*
Coex415-*MAF1*	Coex plasmid harboring P$_{TEF1}$-*MAF1*-T$_{ADH1}$ cassette
Coex415-*tHMG1*	Coex plasmid harboring P$_{TEF1}$-t*HMG1*-T$_{ADH1}$ cassette
Coex415-*tHMG1,ERG20*^{WWG}	Generated by P$_{TDH3}$-*ERG20*^{WWG}-T$_{TPS1}$ cassette insertion in Coex415-thmg1
Coex415-*HMG2*^{K6R}	Coex plasmid harboring P$_{TDH3}$-*HMG2*^{K6R}-T$_{TPS1}$ cassette
Coex415-*ICE2*	Coex plasmid harboring P$_{TDH3}$-*ICE2*-T$_{TPS1}$ cassette

Coex415-*INO2*	Coex plasmid harboring P_{TDH3}-*INO2*-T_{TPS1} cassette
Coex413-*MVD1*	Coex plasmid harboring P_{PGK1}-*MVD1*-T_{PGK1} cassette
Coex415-*ERG10*	Coex plasmid harboring P_{TPI1}-*ERG10*-T_{TPI1} cassette
Coex416-*ERG12*	Coex plasmid harboring P_{PGK1}-*ERG12*-T_{PGK1} cassette
Coex415-*IDI1*	Coex plasmid harboring P_{TEF1}-*IDI1*-T_{ADH1} cassette
Coex414-*ERG13*	Coex plasmid harboring P_{TEF1}-*ERG13*-T_{ADH1} cassette
Coex414-*ERG8*	Coex plasmid harboring P_{TPI1}-*ERG8*-T_{TPI1} cassette
Coex413-t*CrGES*	Coex plasmid harboring P_{TDH3}-*tCrGES*-T_{TPS1} cassette
Coex413-*MsLS*	Coex plasmid harboring P_{TDH3}-*MsLS*-T_{TPS1} cassette
Coex413-t*MsLS*	Coex plasmid harboring P_{TDH3}-*tMsLS*-T_{TPS1} cassette
Coex413-*SdL7H*	Coex plasmid harboring P_{TDH3}-*SdL7H*-T_{TPS1} cassette
Coex415-*PfCPR*	Coex plasmid harboring P_{PGK1}-*PfCPR*-T_{PGK1} cassette
Coex415-*NCP1*	Coex plasmid harboring P_{PGK1}-*NCP1*-T_{PGK1} cassette
Coex413-*SdL7H,PfCPR*	Generated by P_{PGK1}-*PfCPR*-T_{PGK1} cassette insertion in Coex413-*SdL7H*
Coex423-*SdL7H,PfCPR*	Generated by sequential cloning of P_{TDH3}-*SdL7H*-T_{TPS1} and P_{PGK1}-*PfCPR*-T_{PGK1} cassettes into high copy (2µ origin) Coex plasmid
Fusion genes plasmids	
Coex413-$ERG20^{WWG}$-G_6-*tMsLS*	Generated by overlap PCR of insert and cloning into Coex413-P_{TDH3}-X-T_{TPS1} empty vector
Coex413-*tMsLS*-G_6-$ERG20^{WWG}$	
Coex413-$ERG20^{WWG}$-G_6-*tCrGES*	
Coex413-*tCrGES*-G_6-$ERG20^{WWG}$	
Coex413-*SdL7H*-G_6-*46tPfCPR*	
Coex413-*PfCPR*-G_6-*18tSdL7H*	
Coex413-*SdL7H*-G_6-*tMsLS*	
Coex413-*SdL7H*-G_6-$ERG20^{WWG}$-G_6-*tMsLS*	
Coex413-*SdL7H*-G_6-*tMsLS,PfCPR*	Generated by P_{PGK1}-*PfCPR*-T_{PGK1} cassette insertion in Coex413-*SdL7H*-G_6-*tMsLS*
Coex413-*SdL7H*-G_6-$ERG20^{WWG}$-G_6-*tMsLS,PfCPR*	Generated by P_{PGK1}-*PfCPR*-T_{PGK1} cassette insertion in Coex413-*SdL7H*-G_6-$ERG20^{WWG}$-G_6-*tMsLS*
CRISPR/Cas9 plasmids	
Coex413-*CAS9*	Coex plasmid harboring P_{TDH3}-*CAS9*-T_{TPI1} cassette
Coex426-gRNA-perg20	High copy Coex plasmid harboring guide RNA generated by overlap PCR and gRNA structure components
Coex426-gRNA-pmaf1	
Coex426-gRNA-*CIT2*	
Coex426-gRNA-*PAH1*	
Coex426-gRNA-pidi1	
Coex426-gRNA-*YPL062W*	
Coex426-gRNA-H1	
Coex426-gRNA-H2	
Coex426-gRNA-H4	
Coex426-gRNA-H5	
Coex426-gRNA-H7	
Coex426-gRNA-H8	
Coex426-gRNA-delta_int	
Peroxisomal targeting modules plasmids	
Coex413-*MVD1,ERG10,*$ERG20^{WWG}$-G_6-*tMsLS*	

Coex413-*MVD1*-ePTS1,*ERG10*-ePTS1,*ERG20^{WWG}-G$_6$-tMsLS*-ePTS1	Coex plasmid generated by sequential cloning of P$_{PGK1}$-*MVD1*-T$_{PGK1}$, P$_{TPI1}$-*ERG10*-T$_{TPI1}$ and P$_{TDH3}$-*ERG20^{WWG}-G$_6$-tMsLS*-T$_{TPS1}$ cassettes with and without the ePTS1 peroxisomal tag (module 1 Limonene)
Coex413-*MVD1,ERG10,tCrGES-G$_6$-ERG20^{WWG}*	Coex plasmid generated by sequential cloning of P$_{PGK1}$-*MVD1*-T$_{PGK1}$, P$_{TPI1}$-*ERG10*-T$_{TPI1}$ and P$_{TDH3}$-*tCrGES-G$_6$-ERG20^{WWG}*-T$_{TPS1}$ cassettes with and without the ePTS1 peroxisomal tag (module 1 Geraniol)
Coex413-*MVD1*-ePTS1,*ERG10*-ePTS1,*tCrGES-G$_6$-ERG20^{WWG}*-ePTS1	
Coex415-*tMHG1,ERG13,ERG8*	Coex plasmid generated by sequential cloning of P$_{TDH3}$-*tHMG1*-T$_{GPM1}$, P$_{TEF1}$-*ERG13*-T$_{ADH1}$ and P$_{TPI1}$-*ERG8*-T$_{TPI1}$ cassettes with and without the ePTS1 peroxisomal tag (module 2)
Coex415-*tHMG1*-ePTS1,*ERG13*-ePTS1,*ERG8*-ePTS1	
Coex416-*ERG12,IDI1,ERG20^{WWG}*	Coex plasmid generated by sequential cloning of P$_{PGK1}$-*ERG12*-T$_{PGK1}$, P$_{TEF1}$-*IDI1*-T$_{ADH1}$ and P$_{TDH3}$-*ERG20^{WWG}*-T$_{TPS1}$ cassettes with and without the ePTS1 peroxisomal tag (module 3)
Coex416-*ERG12*-ePTS1,*IDI1*-ePTS1,*ERG20^{WWG}*-ePTS1	
Integration plasmids	
CoexH1up-*MVD1*-ePTS1,*ERG10*-ePTS1,*ERG20^{WWG}-G$_6$-tMsLS*-ePTS1-H1down	Coex plasmid without CEN/ARS. Cassettes are flanked by 500 to 700-bp homology arms upstream and downstream the CRISPR/Cas9 cutting site. The homology arms are themselves flanked by SmiI restriction site
CoexH1up-*MVD1*-ePTS1,*ERG10*-ePTS1,*tCrGES-G$_6$-ERG20^{WWG}*-ePTS1-H1down	
CoexH2up-*ERG20^{WWG}-G$_6$-tMsLS*-H2down	
CoexH4up-*tHMG1,ERG20^{WWG}*-H4down	
CoexH4up-*SdL7H,PfCPR*-H4down	
CoexH5up-*tHMG1*-ePTS1,*ERG13*-ePTS1,*ERG8*-ePTS1-H5down	
CoexH7up-*ERG12*-ePTS1,*IDI1*-ePTS1,*ERG20^{WWG}*-ePTS1-H7down	
CoexH8up-*ERG20^{WWG}-G$_6$-tMsLS*-H8down	
CoexH8up-*tCrGES-G$_6$-ERG20^{WWG}*-H8down	

Table 4: Primers used in this study

Primer name	Sequences (forward and reverse) 5'-3'
Gene amplification	
erg20_F,BamHI	gcgGGATCCATGGCTTCAGAAAAAGAAATTAGGAGAGAG
erg20_R,XhoI	gcgCTCGAGTTATTTACTTCTCTTGTAAACCTTGTTCAAAAACGCAG
erg20_R,XbaI	gcTCTAGATTATTTACTTCTCTTGTAAACCTTGTTCAAAAACGCAG
erg20_R,ePTS1-taa-XhoI	gcgTCTAGAttacaatttggatcttctacctcttcccagTTTACTTCTCTTGTAAACCTTGTTCAAAAACGCAG
thmg1_F,ATG,BamHI	gcgGGATCCatgGACCAATTGGTGAAGACTGAAGTCACC
thmg1_R,XhoI	gcgCTCGAGTTAGGATTTAATGCAGGTGACGGACC
thmg1_R,ePTS1-taa-XhoI	gcgCTCGAGttacaatttggatcttctacctcttcccagGGATTTAATGCAGGTGACGGACC
erg10_F,BamHI	gcgGGATCCATGTCTCAGAACGTTTACATTGTATCGAC
erg10_R,XhoI	cgcCTCGAGTCATATCTTTTCAATGACAATAGAGGAAGCACC
erg20_R,ePTS1-tga-XhoI	gcgCTCGAGtcacaatttggatcttctacctcttcccagTATCTTTTCAATGACAATAGAGGAAGCACCACC
erg13_F,BamHI	gcgGGATCCATGAAACTCTCAACTAAACTTTGTTGGTGTG
erg13_R,XhoI	gcgCTCGAGTTATTTTTTAACATCGTAAGATCTTCTAAATTTGTCATCGATG
erg13_R,ePTS1-taa-XhoI	gcgCTCGAGttacaatttggatcttctacctcttcccagTTTTTTAACATCGTAAGATCTTCTAAATTTGTCATCGATG
erg12_F,SpeI	gcgACTAGTATGTCATTACCGTTCTTAACTTCTGCACC
erg12_R,XhoI	cgcCTCGAGTTATGAAGTCCATGGTAAATTCGTGTTTCCTG
erg12_R,ePTS1-taa-XhoI	gcgCTCGAGttacaatttggatcttctacctcttcccagTGAAGTCCATGGTAAATTCGTGTTTCCTG
erg8_F,BamHI	gcgGGATCCATGTCAGAGTTGAGAGCCTTCAG
erg8_R,XhoI	gcgCTCGAGTTATTTATCAAGATAAGTTTCCGGATCTTTTTCTTTC
erg8_R,ePTS1-taa-XhoI	gcgCTCGAGttacaatttggatcttctacctcttcccagTTTATCAAGATAAGTTTCCGGATCTTTTTCTTTCCTAACAC
mvd1_F,BamHI	gcgGGATCCATGACCGTTTACACAGCATCC
mvd1_R,XhoI	gcgCTCGAGTTATTCCTTTGGTAGACCAGTCTTTGCG
mvd1_R,ePTS1-taa-XhoI	gcgCTCGAGttacaatttggatcttctacctcttcccagTTCCTTTGGTAGACCAGTCTTTGCGTC
idi1_F,BamHI	gcgGGATCCATGACTGCCGACAACAATAGTATGC
idi1_R,XhoI	gcgCTCGAGTTATAGCATTCTATGAATTTGCCTGTCATTTTCCAC
idi1_R,ePTS1-taa-XhoI	gcgCTCGAGttacaatttggatcttctacctcttcccagTAGCATTCTATGAATTTGCCTGTCATTTTCCAC
upc2_F,BamHI	gcgGGATCCATGAGCGAAGTCGGTATACAGAATCAC
upc2_R,XhoI	gcgCTCGAGTCATAACGAAAAATCAGAGAAATTTGTTGTTGTCATC
ice2_F,BglII	gcgAGATCTATGACCAGTTTGTCCAAAAGCTTCATG
ice2_R,XhoI	gacCTCGAGTCAACTACCAGAACCTATTAATTCTGTAGCG
ino2_F,BamHI	gcgGGATCCATGCAACAAGCAACTGGGAACG
ino2_R,XhoI	gcgCTCGAGTCAGGAATCATCCAGTATGTGCTGTAGTG
ncp1_F,BamHI	gcgAGATCTCATGCCGTTTGGAATAGACAACACC
ncp1_R,XhoI	gcgCTCGAGTTACCAGACATCTTCTTGGTATCTACCTGAAG
hmg2-K6R-_F,XbaI	gcgTCTAGAATGTCACTTCCCTTAAGAACGATAGTACATTTGG
hmg2_R,XhoI	gcgCTCGAGTTATAATAATGCTGAGGTTTTACAGGGGG

MsLs_F,BamHI	gcgGGATCCATGGCCTTGAAGGTTTTGTCT
tMsLs_F,ATG,BamHI	gcgGGATCCatgAGAAGATCCGGTAATTACAATCCATCAAGA
MsLs_R,XhoI	gcgCTCGAGTCAAGCGAATGGTTCGAACA
MsLs_R,ePTS1-tga-XhoI	gcgCTCGAGtcacaatttggatcttctacctcttcccagAGCGAATGGTTCGAACAAAG
tCrGes_F,ATG,BamHI	gcgGGATCCatgTCCTCGTCGTCCTCGTCCTC
tCrGes_R,SalI	gcgGTCGACTTAGAAGCAAGGGGTGAAGAACAGG
SdL7H_F,BamHI	gcgGGATCCATGGCTGCTTTGTTGTTGCTG
SdL7H_R,XhoI	gcgCTCGAGTTAGTAAGCTCTTGGAGTAGTAACAACCAAC
PfCPR_F,BamHI	gcgGGATCCATGGAATCCACCTCTG
PfCPR_R,XhoI	gcgCTCGAGTTACCAAACATCTCTCAAG
ubi4_F,BamHI	gcgGGATCCATGCAGATTTTCGTCAAGACTTTGACC
ubi4_R,F:K3K15,XhoI	gcgCTCGAGCTTAACCAAAGAAACTGGCAACAACCAAGCACCAGATTTGTG GAAACCACCTCTTAGCCTTAGCACAAG
Genome-editing confirmation	
erg20_R,conf	ACGTTCAAGAATCTCTCTCTCCTAATTTCTTTTTC
H1up800_R,conf	GAACCCACATCAAGCGAATACATACAT
H2up180_F,conf	TCTGATTCCAAGGAGAGTGAAAGAGC
H2down_R,conf	AGTGTCTCCGACGATTTGGATATC
H4up600_F,conf	gttcgttgaccgtatattctaaaaacaagtac
H5up650_F,conf	ACACGCTTGTCCTTCAAGTCCAAATC
H5down275_F,conf	CGTCGATGACTTCCCATACTGTAATTGCTTTTAG
H7up900_R,conf	ACCGATGGTACCAATGATGGAGGTT
H8up200_F,conf	ACTTGTTGCTGCAGAGGAAA
H8down200_R,conf	TGTGCGCCAACCTTTTGATT
cit2-del200_F,conf	GGTGACGTTAATCTAAAGATAGTCATGCTC
cit2-del200_R,conf	GTGATAGCTTCCGCAATTTTCCAACC
pah1-del200_F,conf	GTAGAAGGAAGAGCAAGGACAAGTG
pah1-del200_R,conf	CGAAGAAGTATGTAATTACCAAGTAGCTCAG
phxt1_F,conf	GGGCAGAAGACAGCAAACG
Promoter amplification	
padh1_F,SacI	gcgGAGCTCCGCTCTTTTCCGATTTTTTTCTAAACCG
padh1-R,SpeI	gcgACTAGTTGTATATGAGATAGTTGATTGTATGCTTGGTATAGC
ppgk1_F,SacI	gcTGGAGCTCGAAGTACCTTCAAAGAATGGGGTCTTATCTTG
ppgk1_R,SpeI	gtcaACTAGTTGTTTTATATTTGTTGTAAAAAG
ptef1_F,SacI	AGCTGGAGCTCATAGCTTCAAAATG
ptef1_R,SpeI	gcgGGATCCACTAGTTCTAGAAAACTTAGATTAGATTG
ptpi1_F,SacI	gtcaGAGCTCTATATCTAGGAACCCATCAGG
ptpi1_R,SpeI	gtcaACTAGTTTTTAGTTTATGTATGTGTTTTTTG
ptdh3_F,SacI	GGAGCTCagtttatcattatcaatactcgccatttcaaagaatacg
ptdh3_R,SpeI	cgcACTAGTtcgaaactaagttctggtgttttaaaactaaaaaaaag
perg1_F,NotI	gcgGCGGCCGCTACGTTCGGGATTTAATCTTCTCGCAG
perg1_R,SpeI	gcgACTAGTGACCCTTTTCTCGATATGTTTTTCTGTGATTT
Terminator amplification	
tgpm1_F,XhoI	gtcaCTCGAGGTCTGAAGAATGAATGATTTG
tgpm1_R,NotI	gtcaGGTACCTATTCGAACTGCCCATTCA
tadh1_F,XhoI	gcgCTCGAGGCGAATTTCTTATGATTTATGATTTTTATTATTAAATAAGTTAT AAAAAA
tadh1_R,NotI	gcgGCGGCCGCCCGGTAGAGGTGTGGTCAATAAGAG

tcyc1_F,XhoI	gcgCTCGAGtcatgtaattagttatgtcacgcttac
tcyc1_R,NotI	gcgGCGGCCGCgcaaattaaagccttcgagcg
ttpi1_F,XhoI	gtcaCTCGAGCTAGAAACTAAGATTAATATAAT
ttpi1_R,NotI	gcgGCGGCCGCCAGTTGAAATTTGGATAAGAACATCTTCTCAACG
ttps1_F,XhoI	gcgCTCGAGTGAACCCGATGCAAATGAGACG
ttps1_R,NotI	gcgGCGGCCGCTGTTTCGAAGAAGAGATCAGCGCG
tpgk1_F,XhoI	gcgCTCGAGATTGAATTGAATTGAAATCGATAGATCAATTTTTTTCTTTTC
tpgk1_R,NotI	gcgGCGGCCGCGGCGCGCCATAGGGCGAATTGGGTACCTTTTGTTGCAAGTG GGATGAGCTTG
DpnI mutagenesis	
erg20_F96W_F	TTGAGTTGTTGCAGGCTTACTggTTGGTCGCCGATGATATGATG
erg20_F96W_R	CATCATATCATCGGCGACCAAccaGTAAGCCTGCAACAACTCAATG
erg20_N127W_F	GAAGTTGGGGAAATTGCCATCtggGACGCATTCATGTTAGAGGC
erg20_N127W_R	GCCTCTAACATGAATGCGTCccaGATGGCAATTTCCCCAACTTC
erg20_K197G_F	CACTCCTTCATAGTTACTTTCggtACTGCTTACTATTCTTTCTAC
erg20_K197G_R	GTAGAAAGAATAGTAAGCAGTaccGAAAGTAACTATGAAGGAGTG
upc2_G888D_F	GACGAATACAGTGGAGGTGGTGaTATGCATATGATGCTAGATTTC
upc2_G888D_R	GAAATCTAGCATCATATGCATAtCACCACCTCCACTGTATTCGTC
gRNA primers for CRISPR/Cas9	
gRNA-perg20	GCAGTGAAAGATAAATGATCCCGATAAATAGAGGAAGCAAGTTTTAGAGC TAGAAATAGC
gRNA-pmaf1	GCAGTGAAAGATAAATGATCAATCCGTTTGGAGTAATGAGGTTTTAGAGCT AGAAATAGC
gRNA-cit2	GCAGTGAAAGATAAATGATCGTTAGTTTCATCAATATACGGTTTTAGAGCT AGAAATAGC
gRNA-pah1	GCAGTGAAAGATAAATGATCCTGGACAAGCTGATTCCACGGTTTTAGAGCT AGAAATAGC
gRNA-pidi1	GCAGTGAAAGATAAATGATCAGGTTATTAAGGGCTTCATGGTTTTAGAGCT AGAAATAGC
gRNA-YPL062W	GCAGTGAAAGATAAATGATCTGTTTTTCGACATAAATGAGGTTTTAGAGCT AGAAATAGC
gRNA-H1	GCAGTGAAAGATAAATGATCCCAATGCTAGTAGAGAAGGGGTTTTAGAGC TAGAAATAGC
gRNA-H2	GCAGTGAAAGATAAATGATCAAGATAGGTAAATAAACGCGGTTTTAGAGC TAGAAATAGC
gRNA-H4	GCAGTGAAAGATAAATGATCCCACCATAACATCAATCATGGTTTTAGAGCT AGAAATAGC
gRNA-H5	GCAGTGAAAGATAAATGATCTGGCCCTGATAATAGTATGAGTTTTAGAGCT AGAAATAGC
gRNA-H7	GCAGTGAAAGATAAATGATCGTATCACAACCGACGATCCGGTTTTAGAGCT AGAAATAGC
gRNA-H8	GCAGTGAAAGATAAATGATCTTTTCCCAGAGTACCAGCAAGTTTTAGAGCT AGAAATAGC
gRNA-delta_int	GCAGTGAAAGATAAATGATCGAAACATATAAAACGGAATGGTTTTAGAGC TAGAAATAGC
Donor DNA amplification for CRISPR/Cas9	
cit2-del_F	ATAACAGGTTCTCAAAACTTTTTGTTTTAATAATACTAGTAACAAGAAAATT GGATTACA

cit2-del_R	ATGAGGAAAGAAAAATATGCAGAGGGGTGTAAAAGTAGGATGTAATCCAATTTTCTTGTT
pah1-del_F	TAAGAAACATACAGGGAAGACATTACTGAAGATAGACACATCGGTCGATTAGATTCTTGT
pah1-del_R	CTTAATATGCAGTATGGATCGTTATAAATAATATTCGGCTACAAGAATCTAATCGACCGA
YPL062W-del_F	ATCAGGTCAGGAACTGCCGTCACATACGACACTGCCCCTCACGTAAGGGCCACCGACCAT
YPL062W-del_R	TGAATCCCCCTCACCCCGAATTTATTACGAATTTGCCCACATGGTCGGTGGCCCTTACGT
donor_phxt1_F-1200,perg20-up	GTCCTTATTACTGCGATATACAGTGTGAGGTATTCAACTATTATTCCTCCGAGAAAACCT
donor_phxt1_R,perg20-down	AATCTCTCTCTCCTAATTTCTTTTTCTGAAGCCATGATTTTACGTATATCAACTAGTTGACGATTATGATATC
donor_perg1-ubi-FK3K15_F,perg20up	GTCCTTATTACTGCGATATACAGTGTGAGGTATTCTACGTTCGGGATTTAATCTTCTCGC
donor_perg1-ubi-FK3K15-linker_R,perg20down	AAGAATCTCTCTCTCCTAATTTCTTTTTCTGAAGCGGATCCACCAGAACCCTTAACCAAAGAAACTGGCAACAACCAAG
donorperg1_R,perg20down	AATCTCTCTCTCCTAATTTCTTTTTCTGAAGCCATGACCCTTTTCTCGATATGTTTTTCTGTGATTT
Coex plasmid cloning	
Coex_F,MluI	gactACGCGTGGAACAAAAGCTGGAGCTC
Coex_F,MauBI	GACTCGCGCGCGGGAACAAAAGCTGGAGCTC
Coex_R,AscI-NotI	GACTACGCGTGCGGCCGCTAATGGCGCGCCATAGGGCGAATTGGGTACC
Overlap PCR	
erg20-no-start_F,G6,tCrGes	CTTGCTTCggtggtggtggtggtggtGCTTCAGAAAAAGAAATTAGGAGAGAGAGATTC
CrGes-no-stop_R,G6,erg20	CTGAAGCaccaccaccaccaccaccGAAGCAAGGGGTGAAGAACAGG
tCrGes-no-start_F,G6,erg20	GAAGTAAAggtggtggtggtggtggtTCCTCGTCGTCCTCGTCC
erg20_R-no-stop,G6,CrGes	ACGAGGAaccaccaccaccaccaccTTTACTTCTCTTGTAAACCTTGTTCAAAAACGC
tMsLs_F,G6,no-start,erg20	AGTAAAggtggtggtggtggtggtAGAAGATCCGGTAATTACAATCCATCAAG
erg20_R,G6,no-stop,tMsLs	TCTTCTaccaccaccaccaccaccTTTACTTCTCTTGTAAACCTTGTTCAAAAACGC
erg20_F-no-start,G6,tMsLs	TTCGCTggtggtggtggtggtggtGCTTCAGAAAAAGAAATTAGGAGAGAGAG
MsLs_R-no-stop-G6,erg20	TGAAGCaccaccaccaccaccaccAGCGAATGGTTCGAACAAAG
18tL7H_F,Linker	ATGTTTGGggtggtggtggtggtggtAAAAAATCCCCATCTACTAAGAGGTTG
CPR-no-stop_R,Linker	gatttttttaccaccaccaccaccaccCCAAACATCTCTCAAGTATCTACCGTTC
46tCPR_F,linker	GAGCTTACggtggtggtggtggtggtTTGATGATGATGTTGACTACCTCTGTTG
L7H-no-stop_R,linker	ATCATCAAaccaccaccaccaccaccGTAAGCTCTTGGAGTAGTAACAACC
erg20-no-start_F,G6,L7H	GAGCTTACggtggtggtggtggtggtGCTTCAGAAAAAGAAATTAGGAGAGAGAG

L7H-no-stop_R,G6,erg20	TCTGAAGCaccaccaccaccaccaccGTAAGCTCTTGGAGTAGTAACAACCAAC
tLS-no-start_F,G6,L7H	GAGCTTACggtggtggtggtggtggtAGAAGATCCGGTAATTACAATCCATC
L7H-no-stop_R,G6,tLS	GATCTTCTaccaccaccaccaccaccGTAAGCTCTTGGAGTAGTAACAACCAAC
Quantitative PCR	
act1-qPCR_F	GCCGAAAGAATGCAAAAGGA
act1-qPCR_R	TAGAACCACCAATCCAGACGG

Restriction enzyme sites are underlined

2.3. Quantitative PCR

Following delta-integration, the cassette integration efficiency was measured through quantitative PCR (qPCR) to assess gene copy number. After PCI genomic DNA extraction of the control and sample strains, 5µL of DNA was amplified by a SYBR Green master mix (Roche Life science, Germany) using gene-specific primers and recommendations from the supplier. The qPCR cycle used is as follows: 45 cycles at 95°C for 20s, then 60°C for 20s and 72°C for 20s. The device used was a Lightcycler 480 II (Rock Life science), and crossing points were calculated using the proprietary software. All samples were normalized through *ACT1* house-keeping gene amplification. See Table 4 for the primers used in this experiment.

2.4. GenBank accession numbers

All heterologous genes (Geraniol synthase *CrGES*, accession no. JN882024, *Catharanthus roseus*, (*S*)-Limonene synthase *MsLS*, accession no. L13459, *Mentha spicata*, (*S*)-Perillyl alcohol synthase (or (*S*)-Limonene-7-hydroxylase) *SdL7H*, accession no. MH051318, *Salvia dorisiana*, NADPH-dependent cytochrome P450 reductase (CPR) *PfCPR*, accession no. GQ120439, *Perilla frutescens*) were codon-optimized for *S. cerevisiae* and synthetized by Integrated DNA Technologies IDT (Newark, NJ, USA). Codon-optimized DNA sequences can be found in the *Supplementary Material* section).

2.5. Gene truncation, mutagenesis, and fusion

Several genes were truncated by PCR for an increased catalytic efficiency or stability. A forward primer hybridizing next to the truncated region with an added start codon was used. All gene mutations were performed using a DpnI site-directed mutagenesis protocol [61]. Proper primers (see Table 4) were used for whole plasmid PCR amplification, then the parental plasmid was digested by DpnI. All gene fusions were built by inserting a short flexible GGGGGG (G_6) linker [36] by overlap extension PCR. The ending and starting codons preventing the full-length fused protein synthesis were removed.

2.6. Peroxisomal gene tagging

For the targeting of the whole mevalonate pathway into the peroxisome, all genes were tagged with an enhanced peroxisomal targeting sequence **LGRGRR**-SKL (**e**PTS1) [62] at the end of the gene, as well as the fused (*S*)-limonene or geraniol synthase.

2.7. Culture conditions

Cells were grown in YPD 2% medium or in SC 2% medium lacking the proper amino acid for selective pressure. YPD and SC media were used for strain construction, but SC medium was preferred for monoterpene production, even without plasmid expression (see Fig. S2). Several glucose concentrations were tried, ranging from 20 to 100 g/L.

Cell growth was monitored through optical density (OD) measurements at 600nm with a Varian Cary 50 UV-Vis spectrophotometer (Agilent Technologies, Santa Clara, CA, USA). A typical batch culture consisted of 18mL of medium inoculated to reach a starting OD_{600} of 0.1 in a 100mL Erlenmeyer flask with a seed culture grown overnight in 5mL medium in a 50mL Erlenmeyer flask at 30°C with constant agitation at 170 rpm.

For fed-batch experiments, ethanol feeding was preferred over glucose for monoterpenes production [34], [41], [63]. The initial carbon source was 20 g/L of glucose, and 10 g/L ethanol was fed aseptically after glucose depletion 3 times while monitoring its consumption.

To alleviate the toxicity of the produced monoterpenes and to reduce product evaporation, a 2-layer extractive fermentation strategy was adopted [64]. Dodecane was firstly used as it is a common candidate but was replaced by an isopropyl myristate layer instead for a reduced toxicity [22].

All cultures were done in triplicates.

2.8. Metabolite analysis

Glucose and ethanol from the culture medium were analyzed by high performance liquid chromatography (HPLC) Ultimate 3000 (Thermo Scientific, Dionex, Sunnyvale, CA, USA) equipped with a BioRad Aminex HPX-87H column maintained at a 60°C temperature. 500 µL of medium supernatant was filtered through a 0.22 µm filter and inserted in the device. As a mobile phase, 100% of 5 mM H_2SO_4 in HPLC grade water (Duksan Chemicals, Ansan, Korea) was used at a flow rate of 0.6 mL/min. Metabolites were detected with a refractive index (RI) detector maintained at 35°C.

Target molecules in the organic layer (dodecane or isopropyl myristate) were detected and quantified at the end of the culture. All the culture broth (medium and organic layer) was transferred into a conical tube, then centrifuged at 4°C and 3000 rpm for 5 minutes (Centrifuge 5810R, Eppendorf, Germany) to ensure a proper layer separation. 600 µL of the upper organic layer was filtered and analyzed at a flow rate of 1 mL/min through an Ultimate 3000 reversed-phase HPLC equipped with an Agilent Eclipse XBD-C-18 column maintained at 30°C. All monoterpenoids were detected using the same gradient method, and an Ultimate 3000 UV/Vis

detection system at a wavelength of 210 nm. 2 mobile phases were used to elute the analytes, water (solvent A) and acetonitrile (solvent B) both supplemented with 13 mM of trifluoroacetic acid. A linear gradient (from 0-15 min, 50-80% of solvent B) was followed by a constant 80% of solvent B from 15-18 min, then another linear gradient (18-19 min, 80-50% of solvent B) to end with a steady 50% of solvent B until 19-23 min. Quantifications of all metabolites were done using standard curves with regression values of at least r^2=0.999. Samples were diluted to fall under the linear range interval.

Chapter 3. Results and discussion

Chapter 3. Results and discussion

3.1. Introduction of (*S*)-limonene and geraniol synthases

To produce geraniol, (*S*)-limonene, and subsequently (*S*)-perillyl alcohol, the first step would be to express the proper geraniol and (*S*)-limonene synthases in the *S. cerevisiae* wild-type strain (CEN.PK2-1C) to verify their activity in a heterologous host. The best candidate for geraniol synthesis is the one from the plant *Catharanthus roseus* (*CrGES*) according to previous research [63]. As for (*S*)-limonene, only a few studies referenced its production in *S. cerevisiae*. However, the preferred choice in yeast and *E. coli* hosts is the (*S*)-limonene synthase from *Mentha spicata* (*MsLS*), which has a high enantioselectivity [40]. These two synthases from plant origin have a N-terminal plastid-targeting sequence that will be truncated for an increased activity in microbial hosts. After codon optimization, the two synthases were overexpressed in CEN.PK2-1C using a plasmid vector. 1.17 mg/L of geraniol was produced with *tCrGES* overexpression during a 72-h cultivation period in SC medium (data not shown), but no (*S*)-limonene was detected when t*MsLS* was overexpressed in the WT strain. This is likely due to poor synthase activity and the lack of enough GPP supply (Fig. 2). Therefore, we first focused on increasing the GPP accumulation by monitoring geraniol production with the overexpression of *tCrGES*.

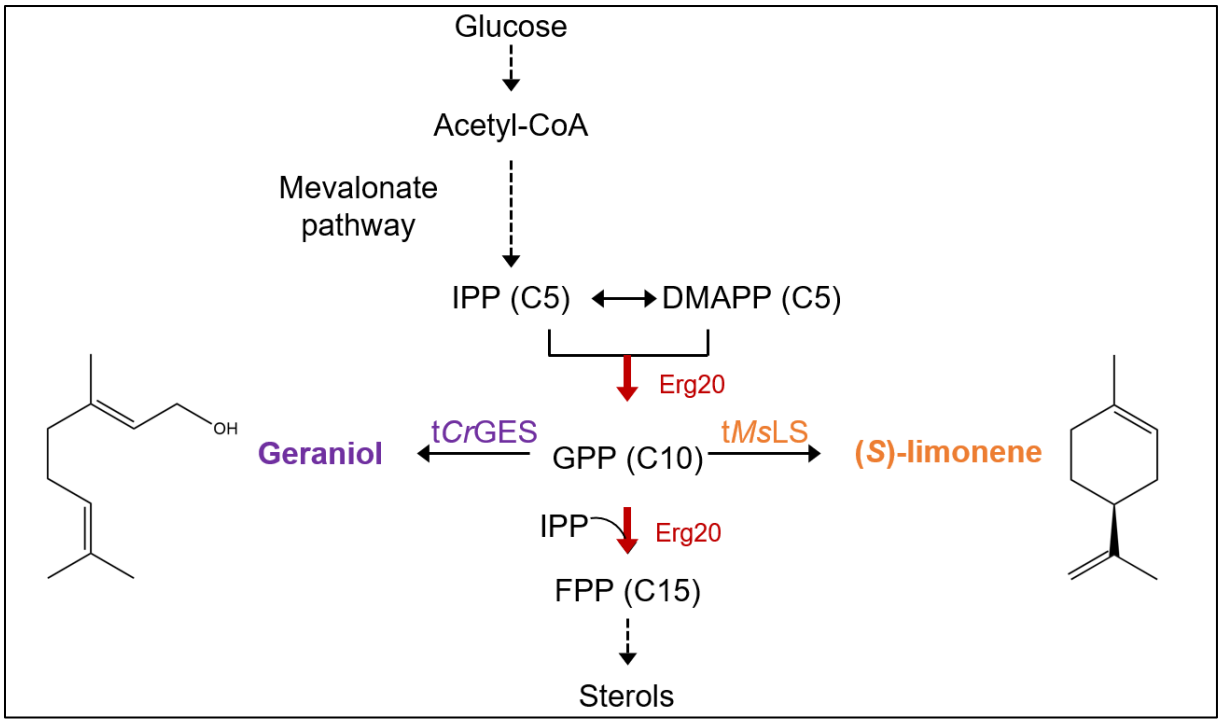

Figure 2: Summarized pathway for geraniol and (*S*)-limonene synthesis in *S. cerevisiae*

3.2. Erg20 mutants for GPP accumulation

The GPP node (Fig. 3A) is critical for GPP accumulation in *S. cerevisiae*. The same enzyme (Erg20) is synthesizing the precursor of monoterpenoids (GPP) from IPP and DMAPP and consumes it to form FPP. Expressing a mutated version of the *ERG20* gene with decreased substrate specificity for GPP is essential to increase the GPP pool. As mentioned earlier, several *ERG20* mutants were discovered, some with better specificity than others. In this study, the two most used mutants (the single mutant K197G and the double mutant F96W N127W), as well as a novel triple mutant combining all of the mutations, were co-overexpressed in the WT strain with *tCrGES* (Fig. 3B). As the geraniol synthase t*Cr*GES consumes GPP to make geraniol, the GPP accumulation level can be indirectly reflected by the geraniol titer at the end of the yeast culture. The best *ERG20* mutant candidate is therefore the one that leads to the best geraniol concentration.

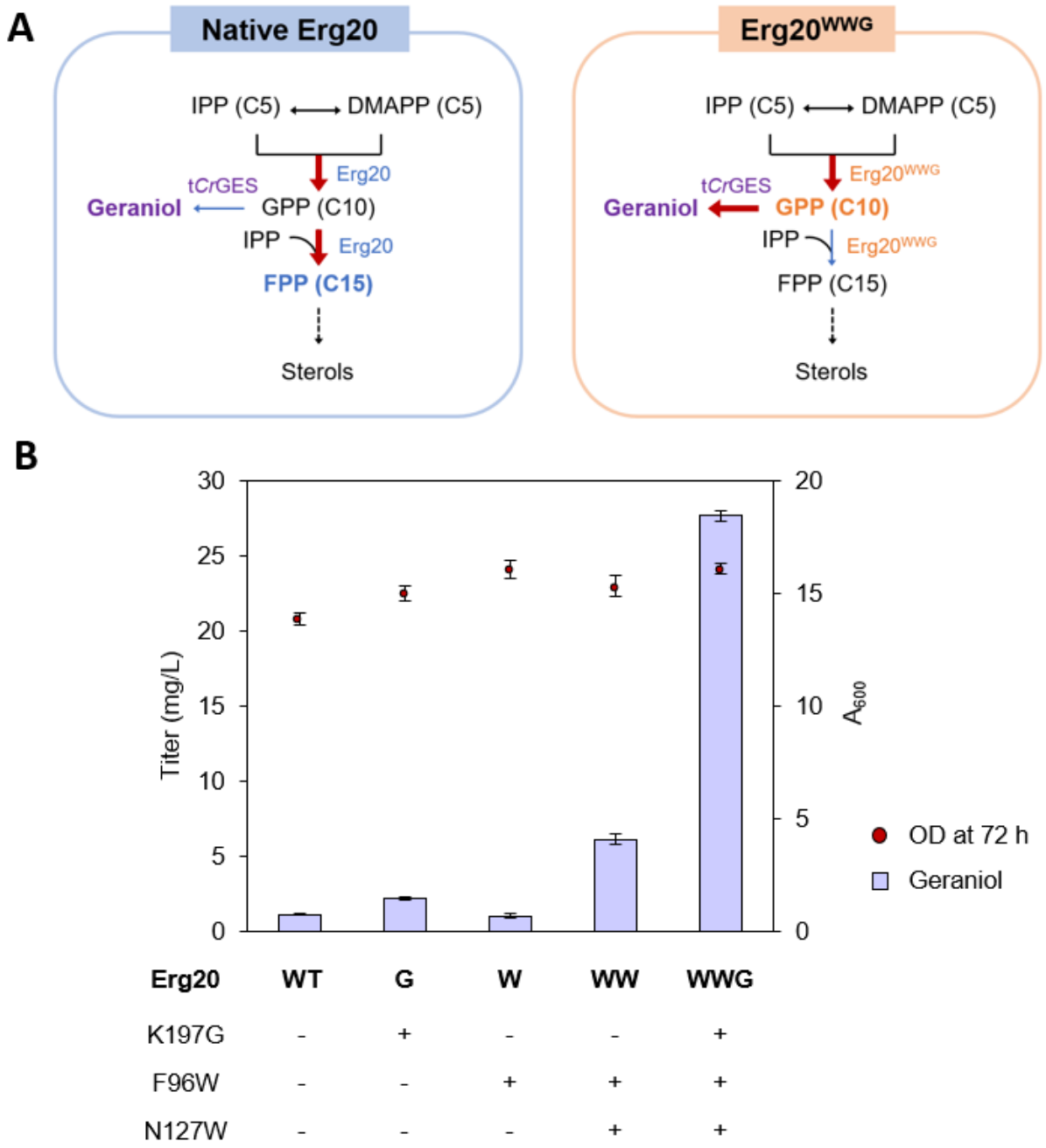

Figure 3: The GPP node and Erg20 mutants for GPP accumulation

A. Representation of the carbon flux at the GPP node with the native Erg20 or the mutated Erg20^{WWG}. **B.** *ERG20* overexpressed on a Coex415 plasmid with no mutation (control), K197G mutation, F96W, F96W and N127W, or all of them at the same time in WT strain. *tCrGES* was overexpressed on a Coex413 plasmid for all samples. Yeasts were cultured in SC medium with 2% glucose lacking histidine and leucine in batch conditions for 72 h.

Except for the F96W single mutant, every other overexpressed mutant increased geraniol synthesis. As expected, the F96W N127W double mutant is superior to the K197G single mutant for GPP accumulation, resulting in a geraniol titer of 6.18 compared to 2.22 mg/L. The novel *ERG20* triple mutant (*ERG20*^{WWG}) is the preferred choice, producing 27.71 mg/L geraniol (nearly a 4.5-fold increase from the double mutant). Its substrate specificity for GPP is greatly reduced compared to the native Erg20. No impact on cell growth was observed, even if the carbon flux going to FPP and sterol synthesis might be lowered when *ERG20*^{WWG} is overexpressed. The basal FPP synthesis ensured by the native *ERG20*, which was not deleted, is likely sufficient to avoid growth impairment. This triple mutant will therefore be co-overexpressed with other key enzymes to ensure a sufficient GPP availability for monoterpenoid synthesis.

3.3. Overexpression of key genes for GPP accumulation and (*S*)-limonene production

Several enzymes are considered rate-limiting in the MVA pathway, such as Hmg1 and Idi1 [31]. To accumulate more GPP, the carbon flux that goes through the MVA pathway must be strengthened by key gene overexpression. Other genes such as the transcription factor *UPC2-1* (*UPC2* with a G888D mutation), which is known to constitutively upregulate sterol synthesis or *MAF1*, responsible for tRNA synthesis downregulation (which uses DMAPP as substrate [30]) might be suitable candidates to strengthen the MVA pathway and reduce the leakage caused by competing pathways. To this matter, truncated *HMG1*, the stabilized mutant of *HMG2* (K6R), *UPC2-1*, *IDI1*, and *MAF1* were co-overexpressed with *tCrGES* to monitor their effect on the MVA pathway and the GPP pool (Fig. 4A).

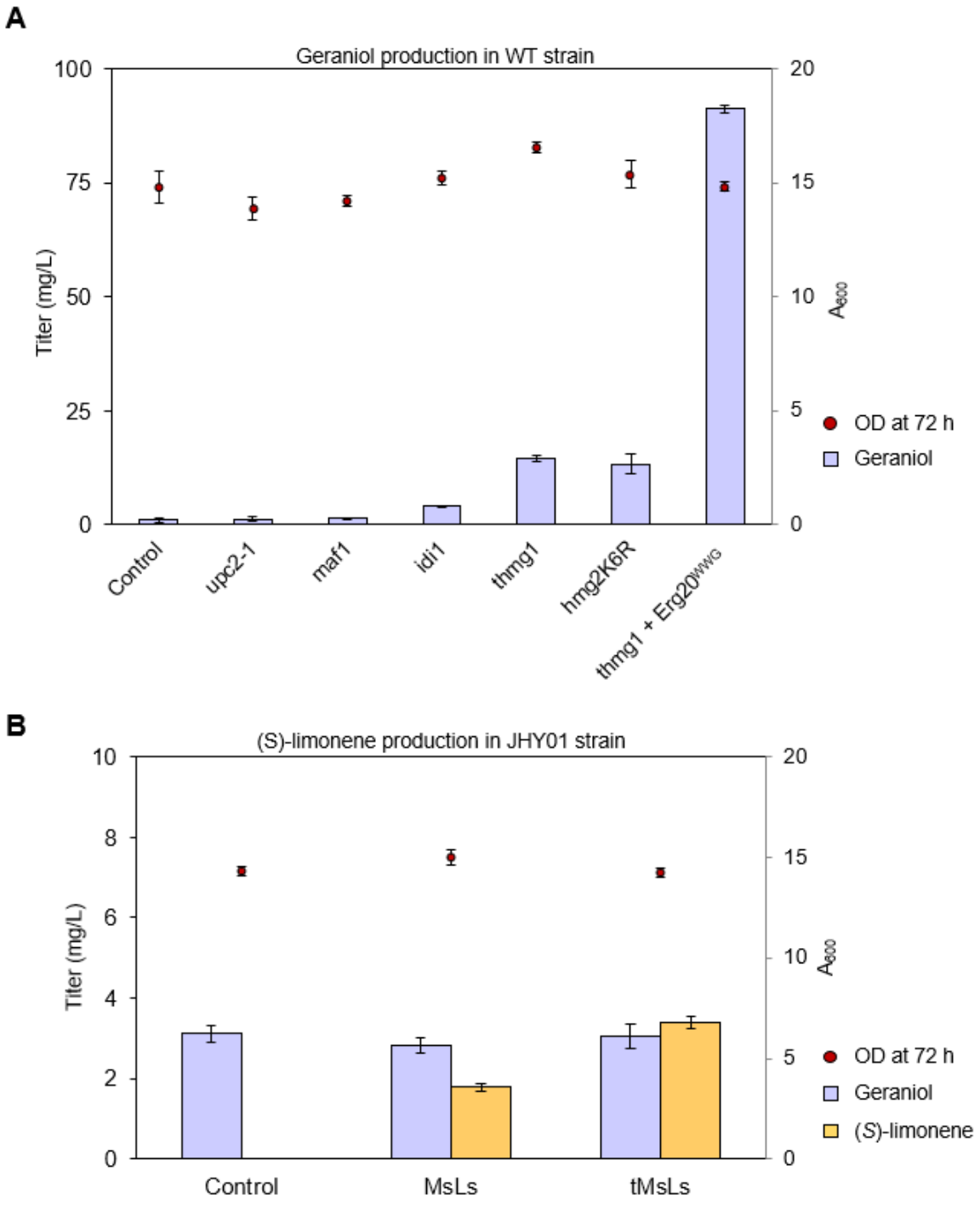

Figure 4: Key genes overexpression for GPP accumulation, and (*S*)-limonene production

A. *tCrGES* co-overexpressed with an empty vector (control), *UPC2-1*, *MAF1*, *IDI1*, *tHMG1*, *HMG2** (K6R) or *ERG20** (WWG) with *tHMG1* in the WT strain. **B.** Empty vector (control), full-length *MsLS* or truncated *MsLS* overexpressed in JHY01 strain. Yeasts were cultured in SC medium with 2% glucose lacking histidine and/or leucine in batch conditions for 72 h.

In Fig. 4A, all the overexpressed genes had little to no impact on cell growth. *UPC2-1* and *MAF1* did not have any significant effect on the GPP accumulation, as the geraniol titers were close to control (1 mg/L in medium). Overexpression of *IDI1* resulted in a 3.8-fold increase (4.05 mg/L). This is likely due to a more optimal DMAPP to IPP ratio, as the native ratio is believed to be suboptimal for monoterpenoid or terpenoid synthesis in general. As Hmg1 is the major bottleneck in the MVA pathway, the most drastic effect on geraniol synthesis happened when truncated *HMG1* or *HMG2** were overexpressed, with 13.7 and 12.5-fold improvement over control (14.6 and 13.4 mg/L). The difference between *tHMG1* and *HMG2** was small, but *tHMG1* was selected for further experiments. When *tHMG1* and *ERG20* triple mutant were both expressed, geraniol titer reached 91.2 mg/L, representing an 85.5-fold improvement compared to the overexpression of *tCrGES* alone. These two genes were then integrated into CEN.PK2-1C genome, resulting in the JHY01 strain. To increase the GPP pool even more, the native *ERG20* was deleted using CRISPR/Cas9 in the JHY01 strain, leaving only *ERG20** (WWG) in the genome, but this deletion was lethal, likely due to insufficient FPP synthesis by the sole triple mutant.

JHY01 was then used to express the (*S*)-limonene synthase (*Ms*LS) to make sure that (*S*)-limonene can be synthetized by using this enzyme in *S. cerevisiae* (Fig. 4B). Both the full-length version and plastid-targeting sequence truncated version were assessed to see if the truncation had a real impact on the catalytic power or stability of *Ms*Ls. Expressing *MsLS* and *tMsLS* resulted in 1.8 and 3.4 mg/L of (*S*)-limonene in the culture medium without significant growth difference. This shows that expressing the truncated monoterpenoid synthase leads to a better titer. In addition, a substantial amount of geraniol (~3 mg/L) was detected at the end of the 72-h batch culture even without expression of the geraniol synthase gene, which was reported previously [65]. It is believed that the accumulated GPP can be hydroxylated by other enzymes, resulting in geraniol production. In this case, if the (*S*)-limonene synthase is

consuming GPP slower than it is produced, GPP accumulates (especially if the native Erg20 is also not producing FPP fast enough). This suboptimal consumption can then result in GPP hydroxylation. This is an issue that has two unwanted outcomes: severe GPP accumulation may be toxic to the cell, and the produced geraniol means that less (*S*)-limonene can be synthetized. Thus, this issue needs to be addressed by enhancing the catalytic power of the (*S*)-limonene synthase. There are several possibilities, such as increasing the gene copy number or performing gene fusion for better substrate availability.

3.4. Protein fusion of t*Cr*GES and t*Ms*LS to Erg20^{WWG} enhances monoterpenoids synthesis

Fusing a heterologous enzyme to the one synthetizing its substrate is a common strategy to enhance its catalytic power [36]. Since a lot of monoterpenoid synthases are suffering from poor catalytic efficiency when expressed in a heterologous host (due to poor substrate availability, suboptimal chemical environment, etc.), co-location of the synthases with Erg20 mutants by protein fusion was tried several times [31], [63]. Geraniol synthases from diverse organisms fused to Erg20^{WW} using several short and flexible protein linkers such as $(G)_6$ or $(G)_4S$ resulted in slight titer increases (1.15 to 1.7-fold depending on the type of geraniol synthase). However, no (*S*)-limonene synthases were fused to Erg20 mutants yet.

In this study, both geraniol and (*S*)-limonene synthases were fused in the N and C-terminal of the novel Erg20^{WWG} by overlapping PCR with the short flexible linker $(G)_6$, and the resulting fused gene was then overexpressed in the GPP-accumulating JHY01 strain (Fig. 5).

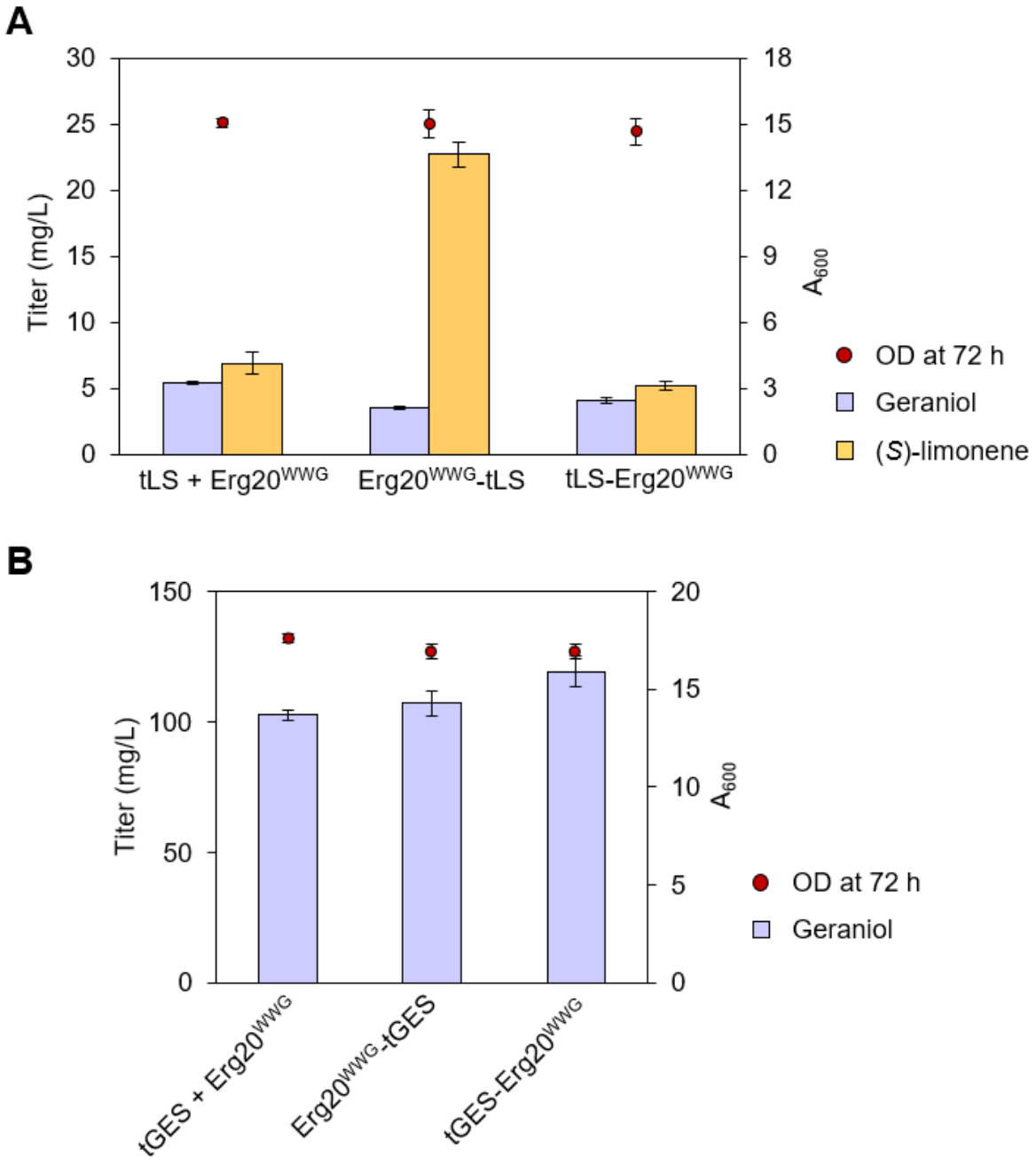

Figure 5: Fused monoterpenoid synthases overexpressed in JHY01 strain

A. Truncated (*S*)-limonene synthase t*Ms*LS fused in N or C-terminal of Erg20^{WWG}. As a control, t*Ms*LS and Erg20^{WWG} are expressed on two different plasmids. **B.** Truncated geraniol synthase t*Cr*GES fused in N or C-terminal of Erg20^{WWG}. As a control, t*Cr*GES and Erg20^{WWG} are expressed on two different plasmids. Yeasts were cultured in SC medium with 2% glucose lacking histidine and leucine in batch conditions for 72 h.

No significant impact on growth was observed in any of the conditions. For (*S*)-limonene, when t*Ms*LS was fused to the C-terminal of Erg20^{WWG}, a significant 3.3-fold improvement in titer was observed compared to the control. In addition, a reduction in geraniol production was noted, indicating the efficient conversion of GPP to (*S*)-limonene prior to its conversion into geraniol through unspecific hydroxylation. However, fusing tMsLS to the N-terminal of Erg20^{WWG} led to a slight titer decrease. This result highlights the impact of protein fusion on the overall protein folding, interactions, and activity. The space conformation of both enzymes is likely bringing the two active sites closer to each other without preventing the substrate to enter or impacting the overall catalysis too much.

For the geraniol synthase, both N and C-terminal fusion increased the geraniol titer but less significantly than the (*S*)-limonene synthase fusions. Fusing t*Cr*GES to the C-terminal or N-terminal of Erg20^{WWG} resulted in a 1.05-fold or 1.16-fold improvement in titer, respectively, compared to the control. Even if the same enzyme Erg20^{WWG} was used as a fusion partner, the ideal orientation for the fusion of t*Ms*LS and t*Cr*GES was found to be opposite to each other. It is likely because the two monoterpenoid synthases have divergent sequences (36.65 % of identity) and structures, their mode of action is different (one hydroxylates GPP and the other cyclizes it) and they are from distinct plant species.

It is noteworthy to say that even if the fusion was more effective for t*Ms*LS, the overall (*S*)-limonene titer is still low (22.71 mg/L) compared to geraniol (107.2 mg/L). Since the geraniol synthase was already quite efficient before the fusion, it is reasonable that fusing it to Erg20^{WWG} did not increase the titer that much compared to t*Ms*LS. As the fusion strategy was efficient for both geraniol and (*S*)-limonene production, those two fused enzymes will then be used in the next metabolic engineering strategy: peroxisomal compartmentalization.

3.5. Peroxisomal compartmentalization of the mevalonate pathway

Compartmentalization strategies are becoming more and more popular in metabolic engineering as they offer many advantages. In *S. cerevisiae,* several organelles might be suitable candidates for monoterpenoid or terpenoid synthesis, such as mitochondria or peroxisomes, especially because of their acetyl-CoA pool. Recently, a wide range of monoterpenoids was produced in peroxisome thanks to the full compartmentalization of the MVA pathway [35]. The obtained titers were several folds higher than cytosolic production and offered other advantages such as an enhanced tolerance to monoterpenoid toxicity and insulation from competing pathways. Also, peroxisomal compartmentalization raised the concentration of precursors, resulting in more efficient monoterpenoid synthesis.

In this study, the whole MVA pathway, as well as the Erg20^{WWG}-fused monoterpenoid synthases, were targeted to the peroxisome in the WT strain by tagging an enhanced peroxisomal-targeting sequence (ePTS1, [62]) (Fig. 6) to the appropriate genes. The 9 genes were overexpressed on 3 different plasmids, with or without the ePTS1 tag to assess the efficiency of compartmentalization on (*S*)-limonene and geraniol titers. ePTS1-tagging permits the migration of newly produced MVA pathway enzymes to peroxisomes. These enzymes are active inside the cytosol during their migration, allowing the utilization of cytosolic acetyl-CoA as well as other precursors. Peroxisomal acetyl-CoA can then be used when the proteins arrive inside peroxisomes. Membrane crossing (Fig. 6A) of precursors is essential because no NADPHs nor ATPs are produced inside the peroxisome despite their utilization in the MVA pathway (2 molecules of NADPH and 3 molecules of ATP are needed to make 1 molecule of GPP). Membrane proteins such as peroxisomal ATP carriers are present on peroxisomes' membranes [66], allowing efficient membrane crossing, which is essential for a feasible peroxisomal production of monoterpenoids.

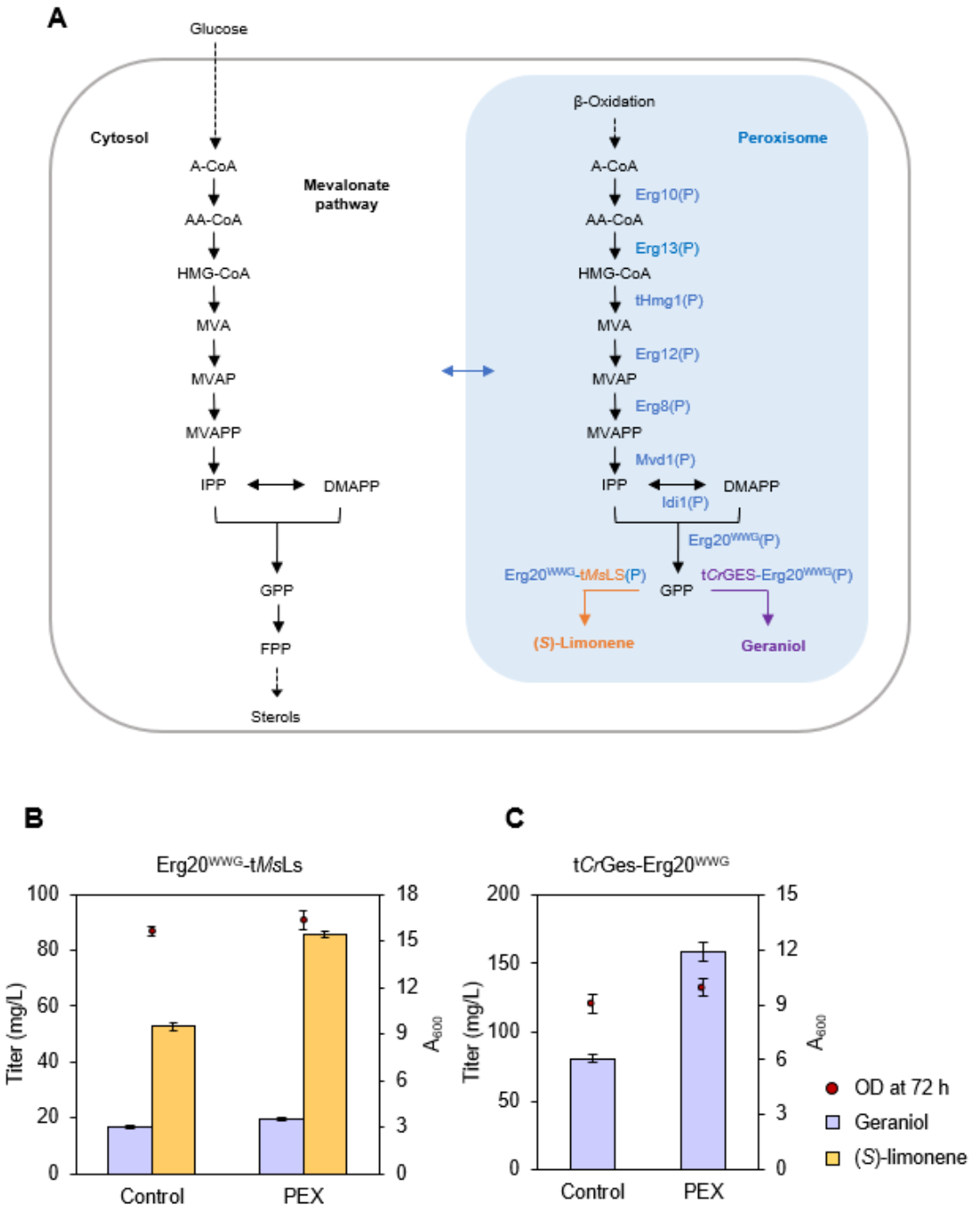

Figure 6: Peroxisomal compartmentalization of the whole mevalonate pathway in the WT strain. **A**. Metabolic pathway overview of the peroxisomal targeting strategy. **(P)** indicates ePTS1-tagging of the MVA pathway genes. The blue double arrow indicates the membrane crossing of molecules between the peroxisome and the cytosol. β-Oxidation refers to the fatty acid oxidation taking place in peroxisomes, resulting in a large pool of acetyl-CoA. **B.** Peroxisomal compartmentalization for (*S*)-limonene production, using the fused Erg20^{WWG}-G$_6$-t*Ms*LS enzyme for (*S*)-limonene synthesis. **C.** Peroxisomal compartmentalization for geraniol production, using the fused t*Cr*GES-G$_6$-Erg20^{WWG} enzyme for geraniol synthesis. Yeasts were cultured in SC medium with 2% glucose lacking histidine, leucine, and uracil in batch conditions for 72 h.

For both (*S*)-limonene and geraniol productions, peroxisomal targeting of the MVA pathway was an efficient strategy, as it increased (*S*)-limonene titer by 1.65-fold (85.62 mg/L) and geraniol titer by 1.96-fold (158.33 mg/L) compared to cytosolic overexpression of the MVA pathway (without the ePTS1 tag).

Also, for (*S*)-limonene synthesis, even if the geraniol titer improved slightly (by 1.16-fold), (*S*)-limonene titer improvement is superior. This means that peroxisomal compartmentalization is efficient not only because it gives access to a new acetyl-CoA pool, but because of other factors. Those are the insulation from competing pathways but also a greater precursor concentration, that increases the overall catalytic power of every enzyme in the MVA pathway, as well as the catalytic efficiency of the (*S*)-limonene synthase, which is rather weak.

No significant growth difference was observed between the cytosolic and peroxisomal monoterpenoid production, but it is worth mentioning that in geraniol peroxisomal production, titers are deceiving compared to the JHY01 strain. The considerable impact on cell growth is likely attributed to the expression of three large plasmids (>12 kb each). The only difference between (*S*)-limonene and geraniol production strains was the fused synthase in one of the plasmids, but the overall growth at the end of the 72-h batch culture was significantly lower in the geraniol-producing strain (9-10 OD_{600} for geraniol to 16-17 OD_{600} for (*S*)-limonene). Indeed, when the peroxisomal modules were integrated into the yeast genome, geraniol titer reached 335.34 mg/L (2.12-fold improvement, Fig. 8B) in SC media, with improved cell growth reaching at an optical density of 17. This titer makes more sense considering the one obtained with JHY01 strain. As for (*S*)-limonene titer, a slight increase to 96.55 mg/L was observed (1.13-fold improvement), without significant cell growth alteration.

Then, two strategies were tried to enhance the overall monoterpenoid production in those peroxisomal compartmentalization strains. Global MVA pathway upregulation by *YPL062W* deletion [67] and peroxisomal acetyl-CoA pool enhancement by *CIT2* deletion [41]. Both deletions were not effective and were therefore abandoned (data not shown).

3.6. (*S*)-Perillyl alcohol production

(*S*)-Perillyl alcohol ((*S*)-POH) is a valuable (*S*)-limonene derivative with potential applications as a drug for cancer treatment and as a bioplastic precursor. It is synthetized by a monooxygenase or hydroxylase that adds a hydroxyl group to the 7th carbon of an (*S*)-limonene molecule. This is performed by a cytochrome P450 enzyme. This monoterpenoid has already been produced in *E. coli* and other prokaryotes using (*S*)-POH synthases from bacterial origin [16]. Recently, a novel (*S*)-limonene-7-hydroxlyase from plant origin has been discovered and expressed in *S. cerevisiae* [48]. A detectable amount of (*S*)-POH has been produced without any by-products, making this cytochrome P450 (CYP) from *S. dorisiana* (*Sd*L7H) a promising candidate. This CYP hydroxylates (*S*)-limonene with a high regiospecificity, something that previously discovered plant (*S*)-POH synthases were not capable of [68]. Most plant CYPs are membrane-bound enzymes, making eukaryotes such as *S. cerevisiae* more suitable cell factories candidates than bacteria [29].

Before expressing *Sd*L7H in *S. cerevisiae*, a major concern needs to be addressed, as CYPs need to be paired with a proper redox partner, a cytochrome P450 NADPH-dependent reductase (CPR), to maintain their catalytic power [29]. There are no known CPRs in *S. dorisiana*, so a partner from a close species will be used instead. Also, no quantified amount of (*S*)-POH was produced in the study where *Sd*L7H was discovered, likely because no CPR was paired with the hydroxylase, resulting in poor catalytic efficiency.

*Sd*L7H shares 70% of identity with a menthofuran from *M. piperita*, 40-65% identity with several hypothetical CYPs from *P. frutescens*, and 40% identity with an unspecific (*S*)-limonene-3/6/7-hydroxylase from *P. frutescens*. In the literature, two main plant CPRs were paired with CYPs that have similar catalytic properties to *Sd*L7H, one from *P. frutescens* [68] and one from *M. spicata* [69]. As a CYP that catalyzes (*S*)-POH formation is already existing in *P. frutescens*, the CPR from this species (*Pf*CPR) was preferred over the other one. This enzyme, as well as *Sd*L7H, were codon optimized, and compared to the native CPR from *S. cerevisiae*, Ncp1 (Fig. 7). All of the (*S*)-POH production strategies were performed in the JHYL04, that produces (*S*)-limonene into yeast peroxisomes.

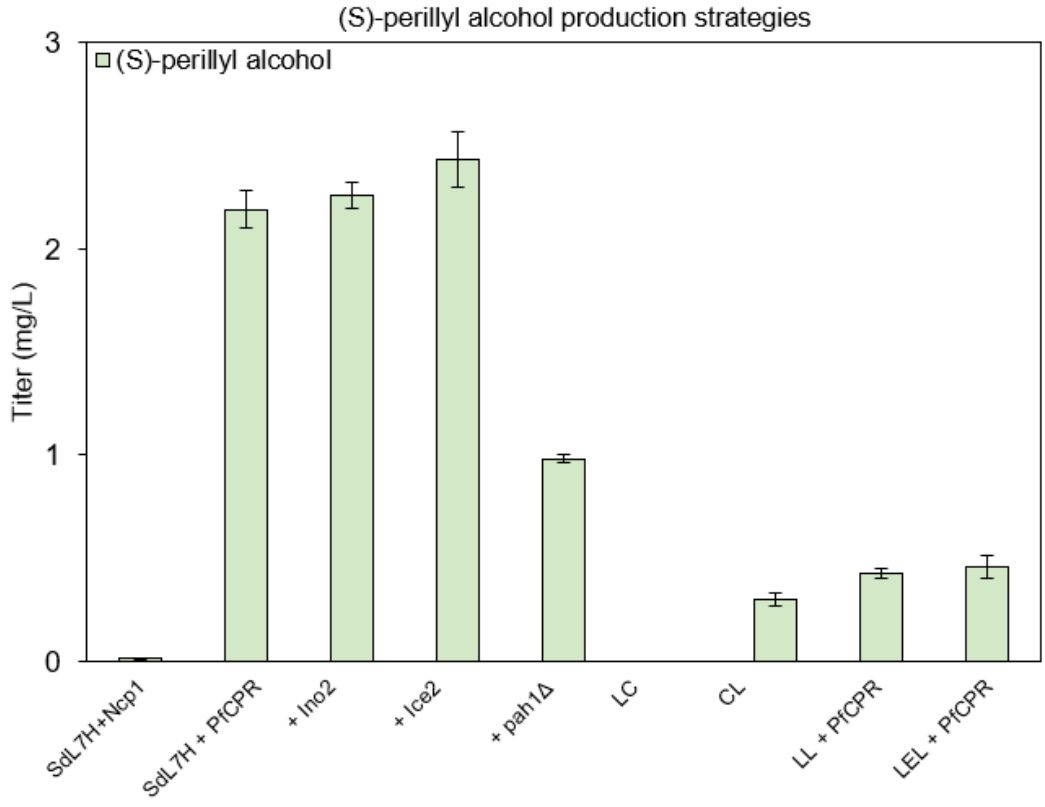

Figure 7: (*S*)-perillyl alcohol production strategies summary in JHL04 strain.

Fused enzymes are abbreviated for clarity purposes. LC: *Sd*L7H-G_6-46t*Pf*CPR. CL: *Pf*CPR-G_6-18t*Sd*L7H. LL: *Sd*L7H-G_6-t*Ms*LS. LEL: *Sd*L7H-G_6-t*Ms*LS-G_6-Erg20^{WWG}. Yeasts were cultured in SC medium with 2% glucose in batch conditions for 72 h, and an isopropyl myristate layer on top of the medium volume to capture monoterpenoids.

When the CPR from *S. cerevisiae* (Npc1) is co-expressed with *Sd*L7H, only a low titer of 13 µg/mL was detected at the end of the 72-h batch biphasic fermentation. When the CPR from *P. frutescens* was expressed instead of Ncp1, (*S*)-POH titer reached 2.19 mg/L, a 178-fold improvement. As a control, no (*S*)-POH was detected when no CPR was co-expressed with the (*S*)-limonene-7-hydroxylase, but the low titer obtained with *NCP1* overexpression might be caused by unspecific (*S*)-limonene hydroxylation, stating that Ncp1 may not act as a redox partner for *Sd*L7H at all. Anyhow, the (*S*)-POH titer obtained with co-expression of *Sd*L7H and *Pf*CPR is also poor compared to the available amount of (*S*)-limonene produced by JHYL04 strain (90 mg/L, Fig 8A). Only 2.4 % of the (*S*)-limonene is converted to (*S*)-POH. Several engineering strategies were tried to address this issue.

As the expansion of the endoplasmic reticulum is a common strategy for enhancing the CYP-CPR expression [29], *INO2* overexpression and *PAH1* deletion were tried without significant titer increase. The overexpression of *ICE2*, which is supposed to reduce heterologous CPR degradation, only resulted in a 1.11-fold improvement over sole *Sd*L7H and *Pf*CPR overexpression in JHYL04 strain. To optimize CYP-CPR interaction, N and C-terminal fusions were tried, in a similar fashion as Erg20^{WWG} and t*Ms*LS fusions. As *Sd*L7H and *Pf*CPR are membrane-bound enzymes, their hydrophobic membrane-binding N-terminal sequences were removed prior to the fusion. This resulted in lower to no (*S*)-POH titer compared to control, likely due to a reduced or loss of activity. A final fusion strategy was performed, with the fusion of the (*S*)-POH synthase to the N-terminal of t*Ms*LS or Erg20^{WWG}-G_6-t*Ms*LS, to ensure better substrate promiscuity with SdL7H (Fig. 7). Even if the final (*S*)-POH titer was higher than previous fusions, it was still lower than unfused *Sd*L7H and *Pf*CPR overexpression. The overall shapes of the fused enzymes might be too different from *Sd*L7H, likely resulting in poor activity of the CPR, that cannot bind to the fused enzymes.

In other microbial (*S*)-POH production studies, one of the main issues was the early extraction of (*S*)-limonene to the organic layer, before its conversion to (*S*)-POH [40]. It is important to mention that a biphasic fermentation strategy is efficient to extract monoterpenoids synthetized directly from GPP but could be a problem for the synthesis of derivatives. The synthesis of (*S*)-POH from (*S*)-limonene in a biphasic culture might be impeded due to early (*S*)-limonene extraction to the organic phase before its utilization by *Sd*L7H.

To address this issue, (*S*)-POH production without any organic layer in the medium was tried, but no product was detected (data not shown). This strategy affected cell growth, likely caused by (*S*)-limonene toxicity, as this monoterpenoid has antifungal activity. An alternative method was tried, with the addition of isopropyl myristate after 48 h of culture, but only a smaller amount of (*S*)-POH than the control was detected and the end of the fermentation (data not shown).

Since most of the engineering strategies failed, two main concerns are believed to be the root of the low (*S*)-perillyl alcohol production. Either the monoterpenoids extraction method is not suitable, or the CYP-CPR pairing was inadequate to begin with. The (*S*)-POH synthase could be poorly expressed in *S. cerevisiae*, resulting in poor titer no matter what the CPR is, or *Pf*CPR might be a poor redox partner choice for *Sd*L7H. Those issues must be addressed to produce (*S*)-perillyl alcohol efficiently, but the focus of this study will shift towards optimization of geraniol and (*S*)-limonene production instead.

3.7. Further strain engineering

3.7.1 Downregulation of wild-type *ERG20*

Expressing a mutated *ERG20* is usually not enough to get an optimal GPP accumulation at the GPP node (Fig. 2). The combination of $Erg20^{WW}$ and native *ERG20* downregulation is a common strategy for producing monoterpenoids in *S. cerevisiae*. Even if the novel $Erg20^{WWG}$ is more efficient to accumulate GPP than the double mutant, native *ERG20* downregulation might still be effective. There are several methods available for the downregulation of essential genes, ranging from switching the native promoter to a leaky or weaker one, to protein destabilization. In this study, 3 methods were tried: the sterol-responsive promoter of *ERG1*, protein destabilization using the N-degron rule, and the glucose-responsive promoter of *HXT1*.

Switching the *ERG20* promoter to P_{ERG1} should decrease the gene expression level when enough ergosterol (essential for growth) is present in the cell, as the *ERG1* promoter is sensitive to ergosterol concentration. Theoretically, when enough carbon flux went to FPP then sterol synthesis, "high" titer of ergosterol will repress the native *ERG20*, resulting in most of the carbon flux going towards monoterpenoid synthesis, as the $Erg20^{WWG}$ enzyme will utilize DMAPP and IPP to mainly form GPP and not FPP.

Downregulation of *ERG20* using the N-degron rule also utilizes P_{ERG1} but with an additional ubiquitin moiety, fused to a N-degron and linked to the start of *ERG20*. After transcription, ubiquitin hydrolysis should reveal the N-degron, leading to early degradation of the Erg20 protein [33].

Firstly, those two strategies were tried for geraniol synthesis on the JHY01 strain (Fig. S1), with slight titer improvements (1.04-fold for P_{ERG1} downregulation and 1.12-fold for the N-degron strategy). These strategies resulted in lower increases than in the literature, but this is likely due to the different types of *ERG20* mutant used (single or double mutants in the literature,

and the triple mutant in this study). Also, the overall carbon flux involved in the MVA pathway might have been too low in the JHY01 strain to see any noticeable effect of the downregulation. Since the N-degron strategy was better than P_{ERG1} promoter swapping alone, it was retried in JHYG06 and JHYL04 strains (geraniol and (*S*)-limonene peroxisomal production strains), alongside downregulation using the *HXT1* promoter (its effect was previously explained).

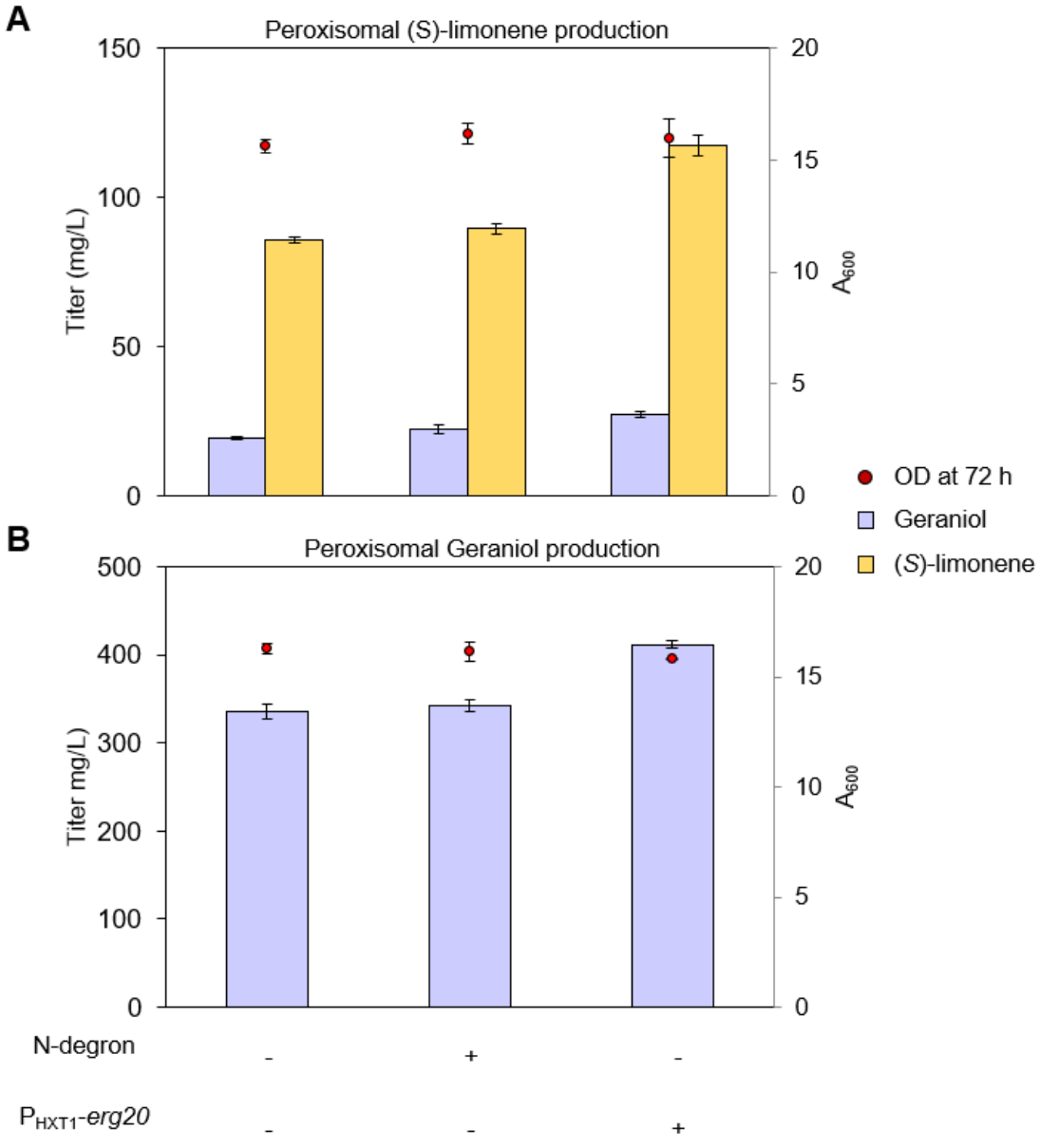

Figure 8: Native *ERG20* downregulation with the N-degron or the P_{HXT1} strategy in peroxisomal compartmentalization strains.
A. *ERG20* downregulation for peroxisomal (*S*)-limonene synthesis in the JHYL04 strain. **B.** *ERG20* downregulation for peroxisomal geraniol synthesis in the JHYG06 strain. Yeasts were cultured in SC medium with 2% of glucose in batch conditions for 72 h.

Overall, the N-degron *ERG20* downregulation was not an efficient strategy for the peroxisomal strains, as only 1.05-fold and 1.02-fold improvements were observed for (*S*)-limonene and geraniol synthesis respectively. Those results are not significant enough to say that this type of downregulation is effective. Also, as the native *ERG20* downregulation takes place in the cytosol, but most of the monoterpenoid synthesis happens in peroxisomes, the downregulation might not be necessary in the first place.

However, using *HXT1* promoter resulted in more significant titer improvements. (*S*)-limonene titer improved by 1.37-fold, and 1.23-fold for geraniol. Even if this downregulation is cytosolic, it likely saves enough GPP, that can be transformed inside the peroxisome after membrane crossing or in the cytosol before MVA pathway enzymes compartmentalization. P_{HXT1} downregulation of native *ERG20* is an effective strategy to accumulate more GPP in batch conditions and might be even more useful in other fermentation conditions, such as fed-batch with ethanol feeding. No significant growth defect was observed with any of the downregulation strategies. As *ERG20* downregulation was effective for both geraniol and (*S*)-limonene production, P_{ERG20} was replaced by P_{HXT1} in JHYG06 and JHYL04 strains, resulting JHYG07 and JHYL05 strains.

3.7.2. Delta-integration of rate-limiting genes

In the global monoterpenoid synthesis pathway, several enzymes are considered to be rate-limiting. In metabolic engineering, overexpression is often not enough to ensure optimal production. In this study, the delta-integration of 3 cassettes was tried to increase the (*S*)-limonene synthesis: *tHMG1*, *ERG20* triple mutant, and the fused *tMsLS*.

Firstly, multicopy delta-integration of one module containing *tHMG1* and *ERG20* triple mutant cassettes, as well as the *TRP1* marker gene was tried in the WT strain. After quantitative PCR, only one copy of the module was integrated. Delta-integration was retried, this time with a shorter module, containing the fused *tMsLs* and *TRP1* marker gene, or the kanamycin resistance gene (under a high antibiotic concentration to facilitate the multicopy integration [70]). Both methods resulted in a single-copy integration into the yeast's genome. The delta-integration was then abandoned in favor of sequential single copy cassette integration by CRISPR/Cas9

3.7.3. Copy number optimization of key genes

A single copy of geraniol and (*S*)-limonene synthases is likely not enough for an optimal GPP conversion to monoterpenoids (especially the (*S*)-limonene synthase as a significant amount of GPP is unspecifically hydroxylated to geraniol). More copies of those fused synthases, as well as an additional copy of *tHMG1* and *ERG20* triple mutant were integrated into JHYG06 and JHYL05 strains to find the optimal copy number (Fig. 9). All additional copies were not targeted to the peroxisomes, as one additional copy of the fused (*S*)-limonene and geraniol synthases targeted to peroxisomes were integrated into both strains, with little to no effect (data

not shown).

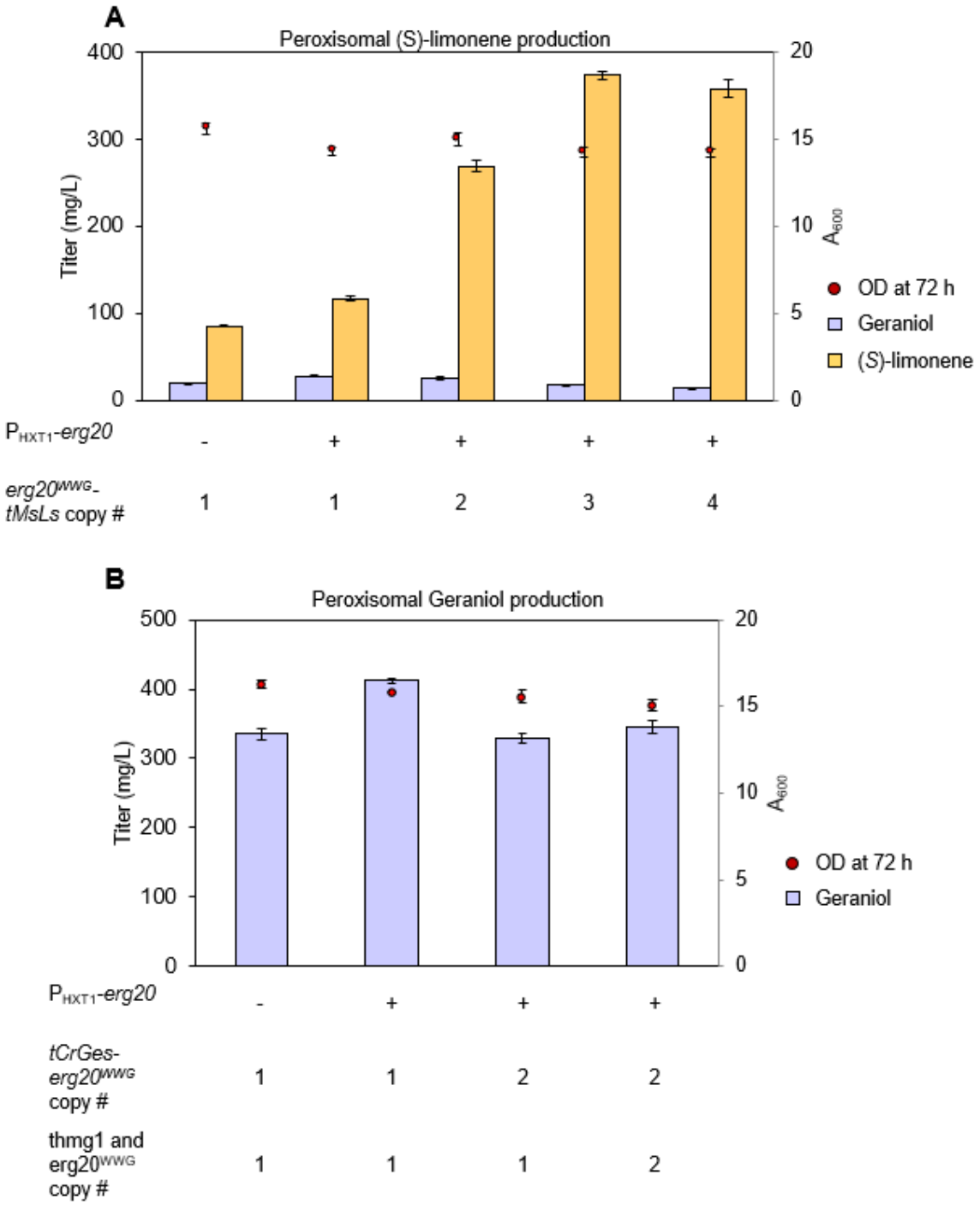

Figure 9: Key genes multicopy integration in JHYG06 and JHYL05 strains.
A. (*S*)-limonene production. Optimization of Erg20^{WWG}-G$_6$-t*Ms*LS copy number. **B.** Geraniol production. Optimization of t*Cr*GES-G$_6$- Erg20^{WWG} as well as tHmg1 and additional Erg20^{WWG} copy number. Monoterpenoids production without *ERG20* downregulation was added to assess the overall titer increase in the peroxisomal compartmentalization strains. Yeasts were cultured in SC medium with 2% in batch conditions for 72 h.

For (*S*)-limonene production, 3 copies of the fused (*S*)-limonene synthase were the optimal choice in these conditions, as an additional 4th copy slightly decreased the titer (the overexpression of too many genes, specifically fused ones that are longer than average, might result in an unwanted metabolic burden on the cell). In batch fermentation, (*S*)-limonene titer reached 374 mg/L in 72-h, a 3.19-fold improvement compared to single copy overexpression. The geraniol titer during (*S*)-limonene production decreased by 1.52-fold from the control, likely due to more GPP being utilized for (*S*)-limonene synthesis rather than unwanted hydroxylation to geraniol. The cell growth decreased slightly with the increasing number of integrated copies, which is reasonable, and either caused by (*S*)-limonene toxicity or the increased metabolic burden. Also, an additional copy of *tHMG1* and *ERG20*^{WWG} were integrated into the strains with 1 or 2 copies of the fused (*S*)-limonene synthase, without any noticeable titer increase (data not shown).

For geraniol synthesis, an additional copy of the fused geraniol synthase decreased the titer by 1.25-fold. An additional copy of *tHMG1* and *ERG20*^{WWG} also resulted in a lower titer than the control. Assuming that the geraniol synthase has a high catalytic power, it is reasonable that overexpression of additional copies did not result in a titer increase. The best geraniol titer is therefore obtained with only one copy coupled to *ERG20* downregulation (411.82 mg/L under a 72-h batch fermentation)

The best (*S*)-limonene titer is almost equivalent to the geraniol one (374 to 411.82 mg/L), which is reasonable because the GPP accumulation level is the same in both strains. Only the type of monoterpenoid synthase and its copy number differs in the two strains. The titer difference might come from the loss of GPP due to its unspecific hydroxylation in the (*S*)-limonene production strain.

3.8. Fed-batch fermentation

After optimizing key genes copy number, the final strains for (*S*)-limonene (JHYL07) and geraniol (JHYG07) were tested in fed-batch conditions. For monoterpenoid production, a fed-batch with ethanol feeding after glucose depletion is a common strategy and has been tried for both (*S*)-limonene [34] and geraniol production [35]. As monoterpenoids are secondary metabolites, their synthesis is favored under partial or total ethanol consumption [41].

Before the fed-batch experiment, rich (YPD) and minimal (SC) media were compared for (*S*)-limonene production (Fig. S2). Even if the OD in the rich medium increased by 1.78-fold, the (*S*)-limonene titer was 2.45-fold higher in the minimal medium. The cell is likely behaving differently in the minimal medium, favoring monoterpenoid production. In the literature, most of the fed-batch experiments were conducted in minimal media. For this fed-batch experiment, SC medium supplemented by 20 g/L of glucose (2%) was used, and 10 g/L of ethanol was added several times after glucose depletion (Fig. 10). The experiment stopped when the cell density started decreasing due to nitrogen (or other nutrients) starvation.

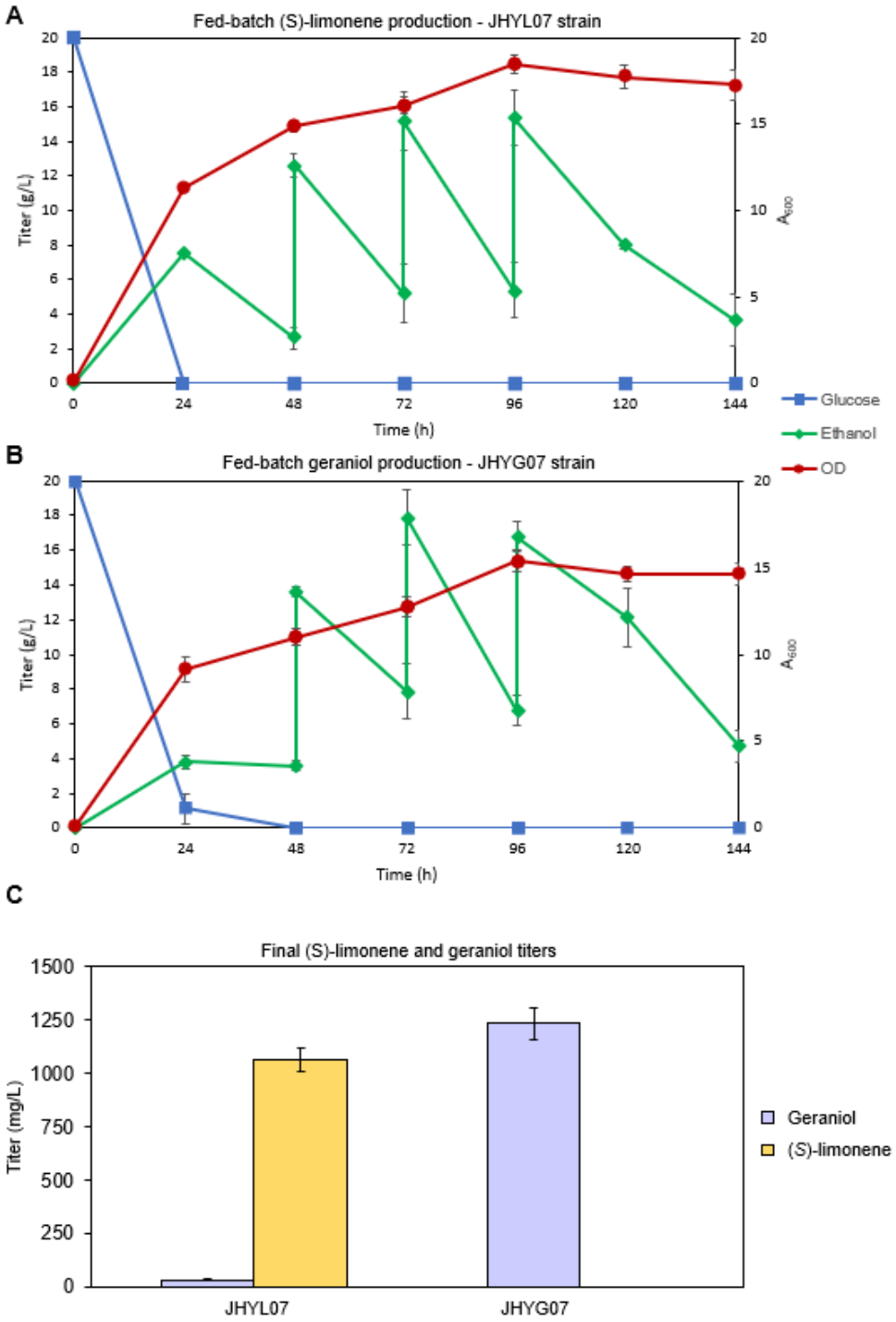

Figure 10: Ethanol-feeding fed-batch experiment using the final (*S*)-limonene and geraniol producing strains.

10 g/L of ethanol was added for both strains at 48, 72 and 96-h. **A.** Time-course variation of the cell density, glucose, and ethanol for the (*S*)-limonene production. **B.** Time-course variation of the cell density, glucose, and ethanol for the geraniol production. **C.** Final titers for both strains after a 144-h fed-batch.

For both strains, 10 g/L of ethanol was added 3 times at 48, 72, and 96 h. For the JHYG07 strain, glucose was not totally depleted at 24 h, likely due to a longer lag phase than JHYL07. Overall, ethanol was well consumed by both strains and was not exceeding 20 g/L in the medium. The growth pattern of the (*S*)-limonene-producing strain was slightly better, reaching 18.5 OD_{600} before the death phase (maximum OD_{600} was 15.87 for the geraniol-producing strain). After the third addition of ethanol, the consumption decreased, as well as the OD, likely due to nitrogen starvation. Assuming that the monoterpenoid production is minimal during this phase, the fed-batch experiment was stopped after 6 days, even if not all the ethanol was consumed by the cells.

At the end of the fed-batch experiment, for JHYL07, the (*S*)-limonene titer reached 1062.96 mg/L with 33.32 mg/l of geraniol as a by-product, a 2.85-fold improvement over a 72-h batch fermentation with the same strain. In the JHYG07 strain, geraniol reached 1233.54 mg/L in the medium, a 3-fold improvement from batch conditions. To the best of my knowledge, this (*S*)-limonene titer is the best achieved in *S. cerevisiae* and yeast hosts in general.

Since only the carbon source was added in this fed-batch experiment, it might be improved by monitoring the pH, aeration, and by adding other nutrients such as a nitrogen source (to optimize the C/N ratio). Also, a scale-up and doing the experiment for a longer period might be necessary to assess the cell viability and the industrial feasibility.

Chapter 4. Conclusion

Chapter 4. Conclusion

In the diverse terpenoid family, monoterpenoids have many valuable uses in nature, have various applications in the cosmetical and pharmaceutical industries, and are an emerging fuel alternative. Due to their versatility, the market demand for monoterpenoids has been growing over the past decades, highlighting the need for a green, stable, and cost-effective synthesis of those molecules, such as microbial production.

The baker's yeast *S. cerevisiae* possesses an efficient endogenous mevalonate pathway, produces naturally high amounts of sterols, and is resistant to toxic chemicals and stressful industrial fermentation conditions, which makes it suitable for large-scale production of monoterpenoids. Regarding monoterpenoid synthesis in *S. cerevisiae*, successful metabolic engineering strategies appeared in recent years but there is still room for improvement, especially for some types of monoterpenoids, such as geraniol, (*S*)-limonene, and their derivatives.

In this study, robust *S. cerevisiae* geraniol and (*S*)-limonene platform strains were built. Those strains reached a gram-scale monoterpenoid titer, making them suitable to produce diverse valuable geraniol and (*S*)-limonene derivatives, such as loganin or (*S*)-perillyl alcohol.

Firstly, a novel $ERG20^{WWG}$ triple mutant was engineered for a better GPP accumulation at the GPP node, crucial for monoterpenoid synthesis. N or C-terminal fusion of this triple mutant to the truncated geraniol or (*S*)-limonene synthase with key genes overexpression resulted in a 22.71 mg/L (*S*)-limonene and a 107.2 mg/L geraniol titer under a 72-h batch extractive fermentation.

Then, peroxisomal compartmentalization of the whole mevalonate pathway as well as the fused monoterpenoid synthases, coupled with native *ERG20* downregulation by the *HXT1* promoter increased the (*S*)-limonene and geraniol titers to reach 117.25 and 411.82 mg/L.

Copy number optimization of the (*S*)-limonene synthase further increased the production, ending with 374 mg/L of (*S*)-limonene under batch fermentation with 3 copies of the synthase. Additional copies of the geraniol synthase or any other key gene did not increase the geraniol production.

The final (*S*)-limonene and geraniol strains were cultured in fed-batch with ethanol addition, reaching gram-scale titers for both strains: 1062.96 mg/L of (*S*)-limonene, the best-achieved titer in a yeast host, and 1233.54 mg/L of geraniol after the 6-days cultivation. Those final titers might be improved by conducting a more complete fed-batch experiment (pH and aeration monitoring, nutrient addition, etc.).

(*S*)-perillyl alcohol production in the (*S*)-limonene platform strain was then tried using a recently discovered plant cytochrome P450 (CYP) paired with a reductase (CPR), reaching a low titer of 2.44 mg/L. Further optimization of the monoterpenoid extraction method or a better CYP-CPR pairing might result in better production.

To increase *(S)*-limonene and geraniol productions even further, several considerations might be addressed, such as product toxicity and the extractive fermentation process. Also, a stronger cofactor supply and balancing, as well as an optimization of the peroxisomal production strategy through more strain engineering might enhance the overall production. Since a lot of genes are overexpressed in the final platform strains, another approach such as dividing the labor in a synthetic consortia strategy might reduce the overall metabolic burden.

Supplementary material

Table S1: DNA sequences of codon-optimized heterologous genes used in this study

Gene name	Sequence (5'-3')	Reference
Geraniol synthase *CrGES* JN882024	ATGGCCGCCACTATCTCTAACCTGTCTTTCCTGGCCAAGTCTCGAGCCCTGTCTCGACCCTCTTCTTCTTCTCTGTCT TGGCTCGAGCGACCCAAGACCTCTTCTACCATCTGTATGTCTATGCCCTCTTCCTCGTCGTCCTCGTCCTCTTCGTCT ATGTCTCTGCCCCTGGCTACCCCTCTGATCAAGGACAACGAGTCCCTGATCAAGTTCCTGCGACAGCCCCTGGTGC TGCCCCACGAGGTGGACGACTCTACCAAGCGACGAGAGCTGCTGGAACGAACCCGAAAGGAACTCGAGCTGAAC GCCGAGAAGCCCCTCGAGGCCCTGAAGATGATCGACATCATCCAGCGACTGGGCCTGTCTTACCACTTTGAGGAC GACATCAACTCTATCCTGACCGGCTTCTCTAACATCTCTTCGCAGACCCACGAGGACCTGCTGACCGCCTCTCTGT GCTTCCGACTGCTGCGACACAACGGCCACAAGATCAACCCCGACATCTTCCAAAAGTTCATGGACAACAACGGCA AGTTCAAGGACTCTCTGAAGGACGACACCCTGGGCATGCTGTCTCTGTACGAGGCCTCTTACCTGGGCGCCAACG GTGAAGAGATCCTGATGGAAGCCCAAGAGTTCACCAAGACTCACCTGAAGAACTCGCTGCCCGCCATGGCTCCCT CGCTGTCTAAGAAGGTGTCTCAGGCCCTCGAGCAGCCCCGACACCGACGAATGCTGCGACTCGAGGCTCGACGAT TCATCGAGGAATACGGCGCCGAGAACGATCACAACCCTGACCTGCTCGAGCTGGCCAAGCTGGACTACAACAAGG TGCAGTCTCTGCACCAGATGGAACTGTCTGAGATCACCCGATGGTGGAAGCAGCTGGGCCTCGTGGACAAGCTGA CCTTCGCTCGAGATCGACCCCTCGAGTGCTTCCTGTGGACCGTGGGACTGCTGCCCGAGCCTAAGTACTCTGGCTG CCGAATTGAGCTGGCTAAGACCATTGCCATCCTGCTGGTGATCGACGACATTTTCGACACCCACGGCACCCTGGAC GAGCTGCTGCTGTTCACCAACGCCATCAAGAGATGGGACCTCGAGGCTATGGAAGATCTGCCCGAGTACATGCGA ATCTGCTACATGGCCCTGTACAACACCACCAACGAGATCTGTTACAAGGTGCTGAAGGAAAACGGCTGGTCTGTT CTGCCCTACCTGAAGGCCACCTGGATCGACATGATCGAGGGCTTCATGGTCGAGGCCGAGTGGTTCAACTCTGACT ACGTGCCCAACATGGAAGAATACGTCGAGAACGGCGTGCGAACCGCCGGCTCTTACATGGCTCTGGTGCACCTGT TCTTTCTGATCGGCCAGGGCGTGACCGAGGACAACGTGAAGCTGCTGATCAAGCCCTATCCTAAGCTGTTCTCTTC TTCCGGCCGAATCCTCCGACTGTGGGACGACCTGGGCACCGCCAAGGAAGAACAAGAGCGAGGCGACCTGGCCTC TTCCATCCAGCTGTTCATGCGAGAGAAGGAAATCAAGTCTGAGGAAGAAGGCCGAAAGGGCATCCTCGAGATCAT CGAGAACCTGTGGAAGGAACTGAACGGCGAGCTGGTGTACCGAGAGGAAATGCCTCTGGCCATCATCAAGACCG CCTTCAACATGGCCCGAGCTTCTCAGGTGGTGTACCAGCATGAGGAAGATACCTACTTCTCTTCTGTGGACAACTA CGTGAAGGCCCTGTTCTTCACCCCTTGCTTCTAA	[71]
(*S*)-Limonene synthase *MsLS* L13459	ATGGCCTTGAAGGTTTTGTCTGTTGCTACTCAAATGGCTATCCCATCTAATTTGACTACTTGCTTGCAACCCTCTCA CTTCAAATCTTCTCCAAAGTTGTTATCCTCCACCAACTCTTCATCAAGATCCAGATTGAGAGTCTACTGCTCATCTT CTCAATTGACTACCGAAAGAAGATCCGGTAATTACAATCCATCAAGATGGGATGTCAACTTCATCCAGTCTTTGTT GTCCGATTACAAAGAAGATAAGCACGTTATCAGAGCCTCTGAATTGGTTACTTTGGTCAAGATGGAATTGGAGAA AGAAACCGACCAAATCAGACAGTTGGAATTGATTGATGACTTGCAGAGAATGGGTTTGTCCGATCATTTTCAGAA CGAGTTCAAAGAGATCCTGTCCTCTATCTACTTGGATCATCATTACTACAAGAACCCATTTCCAAAAGAAGAGAGG GACTTGTACTCTACTTCTTTGGCTTTCAGACTGTTGAGAGAACATGGTTTTCAAGTTGCCCAAGAAGTTTTCGACTC TTTCAAGAATGAAGAGGGCGAATTCAAAGAGTCTTTGTCTGACGATACAAGAGGTTTGTTGCAGTTGTATGAAGC CTCATTCTTGTTGACTGAAGGTGAAACTACTTTGGAATCCGCTAGAGAATTTGCTACCAAGTTCTTGGAAGAAAAG GTTAACGAAGGTGGTGTTGATGGTGATTTGTTGACTAGAATTGCCTACTCCTTGGATATTCCATTGCATTGGAGAA TCAAAAGACCAAATGCTCCAGTTTGGATCGAGTGGTATAGAAAAAGACCAGATATGAACCCAGTCGTTTTGGAAT TGGCTATCTTGGATTTGAACATCGTCCAAGCACAATTCCAAGAAGAGTTGAAAGAATCATTCAGATGGTGGCGTA ATACCGGTTTTGTTGAAAAATTGCCATTCGCCAGAGATAGATTGGTTGAATGTTACTTTTGGAACACCGGTATCAT CGAACCTAGACAACATGCTTCTGCTAGAATCATGATGGGTAAAGTTAACGCCTTGATCACCGTTATCGATGATATC TATGATGTTTACGGCACCTTGGAGGAATTGGAACAATTCACTGATTTGATCAGAAGGTGGGACATCAACTCTATAG ATCAATTGCCAGACTACATGCAGTTGTGTTTCTTGGCATTGAACAACTTCGTTGATGATACCTCCTACGACGTCAT GAAAGAAAAGGGTGTTAACGTTATCCCATACTTGAGACAATCTTGGGTTGATTTGGCTGATAAGTACATGGTTGA AGCTAGATGGTTTTACGGTGGTCATAAGCCATCTTTGGAAGAATACTTGGAAAACTCCTGGCAGTCTATTTCTGGT CCATGTATGTTGACCCATATCTTCTTCAGAGTTACCGACTCCTTTACCAAAGAAACTGTTGACTCCTTGTACAAATA CCACGATTTGGTTAGATGGTCCTCATTCGTTTTGAGATTGGCAGATGATTTGGGTACTTCTGTTGAAGAGGTTTCTA GAGGTGATGTTCCAAAGTCCTTGCAATGTTACATGTCTGATTACAACGCTTCTGAAGCTGAAGCAAGAAAACATGT TAAGTGGTTGATTGCCGAAGTCTGGAAAAAGATGAATGCCGAAAGAGTTTCTAAGGACTCTCCATTTGGTAAGGA TTTCATTGGTTGTGCTGTTGACTTGGGTAGAATGGCTCAATTGATGTACCATAATGGTGATGGTCATGGTACTCAA CATCCAATTATCCATCAACAGATGACCAGAACTTTGTTCGAACCATTCGCTTGA	[72]
(*S*)-Perillyl alcohol synthase (or (*S*)-Limonene-7-hydroxylase	ATGGCTGCTTTGTTGTTGCTGATCTCTTTCATGTTCTTGGTCCTGTTCTTCTTCAAAAAATCCCCATCTACTAAGAGG TTGCCACCATCTCCATTGAAGTTGCCAATTATTGGTAACATCTACTTGGCTGGTTCTTTGCCACATAGATCTTTCCA ATCTTTGTCCAAGAGATACGGTGAAGTTATGTTGTTGCATTTCGGTTCTAAGCCAGTTGTTGTAGCTTCTTCTGCTA ATGCTGCTAGAGAAATTATGAAGAACCAGGATTTGATCTTCGCCTCTAGACCAAGATTGTCCTTCATTGATAGATT CTTCTACGGTGGTAGAGATGTTGCTTTTGCTGCTTATGGTGATTCTTGGAGAAAAGGTAGATCAATGTGTGTCTTG CACCTGTTCTCATCTAAGAGAGTTCAATCCTTCAGACCAATCAGAGATGAAGAAACCTCTTTGATGATCGAGAAG ATCAAGAGATCTTCCCCATCTGTTGTTAACTTGTCCGAAATGTTCATGTCCTTGACCAACGATGTTGTTTCTAGAGC TGTTTTGGGTAGAACTTATGGTGGTGATGATGACGGTGAAAAGAACTTCAATCAGATCCTGAAGAAGATCGTCGA AATCTTGCAATCTTACAACGTTGGTGATTTCGTTGCTTGGTTAGGTTGGATTAACAGAGTTAATGGTGTTGAAGCC CAAGTCGAAAAGATTTTCGAAATGACTGACGAATTCATGGAAGCCTTGTTGAGAGAGTATAGGGACAAGAAATCT TCTGGTGATGCCGTTGTTAATTTCGCTGATGCTTTGTTAGAATTGCAGGGTGAATCTAAGGATTCCGATCCAGTTG AAGATGATGTTATTAAGGCCTTGATCTTGGATACTTTCGCTGCTGGTACTGATACAACTTTTACTGCTTTGGAATGG ACCATGGCCGAATTGATTAGAAATCCTAGAACCATGAAGCTGTTGCAGAAAGAAGTTAGAGAAGTTGCTAGGAAC AAGAACGGTATCGATATCAACGAAGATGACTTGGAAAAGATGCCATACTTGAAGGCCGTTTCCAAAGAATCTTTG	[48]

) *SdL7H* MH051318	AGATTGCATCCACCATTGCCATTGGCTTTACCAAGAGAATTGAATCAAGACACCAACTTGTTGGGTTACGATATTC CAAGAGGTGCTTTGGTTTTGGTTAACTGTTGGGCTATTTCTAGAGATCCTTTGTTGTGGGAAAACCCAAATGAATT CAGACCAGAAAGGTTCTTCGACTCCTCTATTGATTACAAGGGCTTGCACTTTGAAATGGTTCCATTTGGTGCTGGT AGAAGAGGTTGTCCAGGTATTGCATTTGCTATGTCTATGTACGAATTGGCCGTTTCTAGATTGGTCAAAGAATTCG ATTTTGGTTTGCCAAACGGTGTCAGAGAAGAGGATTTGGATATGACTGAAGCTCCAGGTTTTGTTGTTCATAAGAA GTCACCTTTGTTGGTTGTTACTACTCCAAGAGCTTACTAA	
NADPH-dependent cytochrome P450 reductase (CPR) *PfCPR* GQ120439	ATGGAATCCACCTCTGAAAAGTTGTCTCCATTTGATTTCATGGCCGCTATTTTGAAGGGTGTTAAGTTGGATACTTC TAACGGTTCTGCTGGTGCTGCTCAACCAGCTGTTGTTGCTATGTTGATGGAAAACAGAGACTTGATGATGATGTTG ACTACCTCTGTTGCTGTTTTGTTGGGTTGTGTTGTTTACCTGATTTGGAGAAGAGGTACTGGTTCTGCTAAAAAGGT TGTTGAACCACCAAAATTGGTTGTTACAAAAGCTCCAGCTGAAACCGAAGAGGTTGATGATGGTAAAAAGAAGGT TACCATCTTCTTCGGTACTCAAACTGGTACTGCTGAAGGTTTTGCTAAAGCTTTGGCTGAAGAAGCTAAAGCTAGA TATCCACAAGCTAACTTCAAGGTTGTCGATTTGGATGATTATGCTGCCGATGATGAAGAATACGAAGAGAAGATG AAGAAAGAGTCCTTCGCTTTCTTTTTCTTGGCTACTTATGGTGATGGTGAACCTACTGATAATGCTGCTAGATTTTA CAAGTGGTTCGCCGAAGGTAAAGAAAGGGGTGATATGTTTAAGAACTTGCACTACGGTGTTTTCGGTTTGGGTAA TAGACAATACGAACACTTCAACAAGATCGCCATTGTCGTTGATGATATTTTGGCAGAACAAGGTGGTAAGAGATT GGTTTCTGTTGGTTTGGGTGATGATGACCAATGTATCGAAGATGATTTTTCCGCTTGGAGAGAAAATGTTTGGCCA GAATTGGATAAGATGTTGAGGGATGAAGATGATGCTACTGTTTCTACTCCATATACTGCTGCTGTTTTAGAGTACA GAGTTGTTTTCCACGATCAATCCGATGGTTTGTCCTCAGAAAATTCTTTGGCTAATGGTCATGCTAACGGTATTGCT GCTTATGATGCTCAACATCCAGTTGTTGCAAATGTTGCCGTTAAGAAAGAATTGCATACCCCATTGTCTGATAGAT CTTGTACCCATTTGGAATTCGACATTTCTGGTTCTGGTTTGGAATACGAAACTGGTGATCATGTTGGTGTTTACTGC GAAAACTTGATCGAAACTGTTGAAGAAGCCGAAAGATTATTGGGTATGCCACCACAAACTTACTTCTCTGTTCATA CCGACAAAGAGGATGGTACTCCATTGGGTGCTTTGCCACCACCATTTCCACCATGTACTTTGAGAACTGCTTTGTC TAGATACGCCGATTTGTTGAATGCTCCAAAGAAATCTGCTTTGACTGCTTTAGCTGCTTACGCTTCTGATCCATCTG AAGCTGATAGATTGAAACATTTGGCTTCTCCAGCTGGTAAAGAAGAGTACGCTCAGTATATCGTTGCTGGTCAAA GATCCTTGTTGGAAGTTATGACTGATTTCCCATCTACTAAGCCACCATTAGGTGTTTTCTTTGCTGCTATTGCTCCA AGATTGCAACCTAGATTCTACAGCATTTCCTCCTCTCCAAAAATTGCCCACTCTAGAATTCATGTTACCTGCGCTTT GGTTTACGAAAAGACTCCAACTGGTAGAATCCATAAGGGTGTTTGTTCTACTTGGATGAAGGATGCTGTTCCATTG GAAGAATCTCCAAACTGTTCTTCTGCTCCAATTTTCGTTAGAACCTCCAATTTCAGATTGCCAGCTGATCCAAAAG TTCCCATTATTATGATTGGTCCAGGTACAGGTTTGGCTCCTTTTAGAGGTTTCTTACAAGAAAGGTTGGCCTTGAAA GAATCTGGTGCTGAATTGGGTCCAGCTATTTTGTTTTTCGGTTGCAGAAACTCCAAGATGGACTTCATATACGAAG ATGAGTTGAACCATTTCGTTAAGGCTGGTGTTGTTTCCGAATTGGTTTTGGCTTTTTCTAGAGAAGGTCCCACCAAA GAATACGTTCAACATAAGATGGCTCAAAAGGCTTTGGATTTGTGGAACATGATTTCTGAAGGTGGTTACGTTTATG TTTGCGGTGATGCTAAAGGTATGGCTAGAGATGTTCATAGAACCTTGCATACCATCGTTCAAGAACAGGGTTCTTT GGATTCCTCTAAGACTGAATCCTTTGTCAAGAACCTGCAAATGAACGGTAGATACTTGAGAGATGTTTGGTAA	[68]

Underlined parts show the truncated DNA sequence

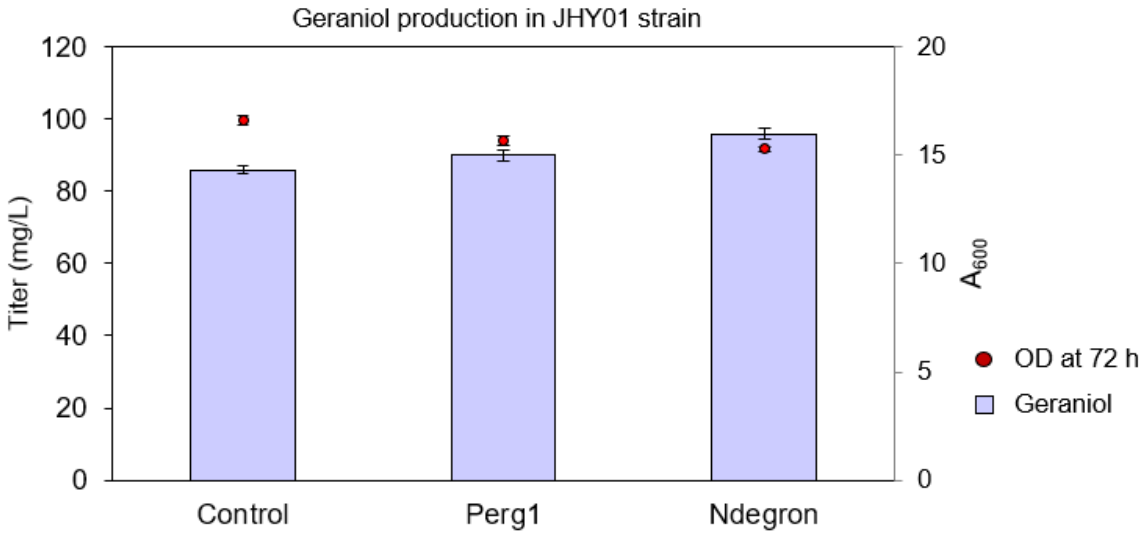

Figure S1: Native *ERG20* downregulation strategies in JHY01 strain. Yeasts were cultured in SC medium with 2% of glucose in batch conditions for 72 h.

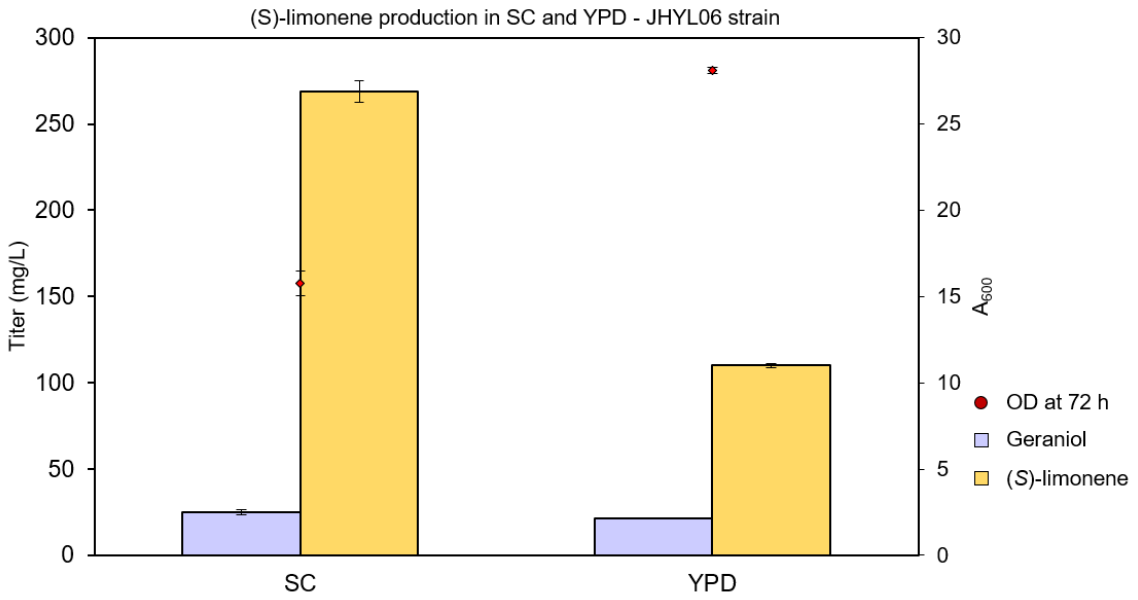

Figure S2: Rich and minimal media comparison for (*S*)-limonene production in JHYL06 strain. Yeasts were cultured in SC medium with 2% of glucose in batch conditions for 72 h.

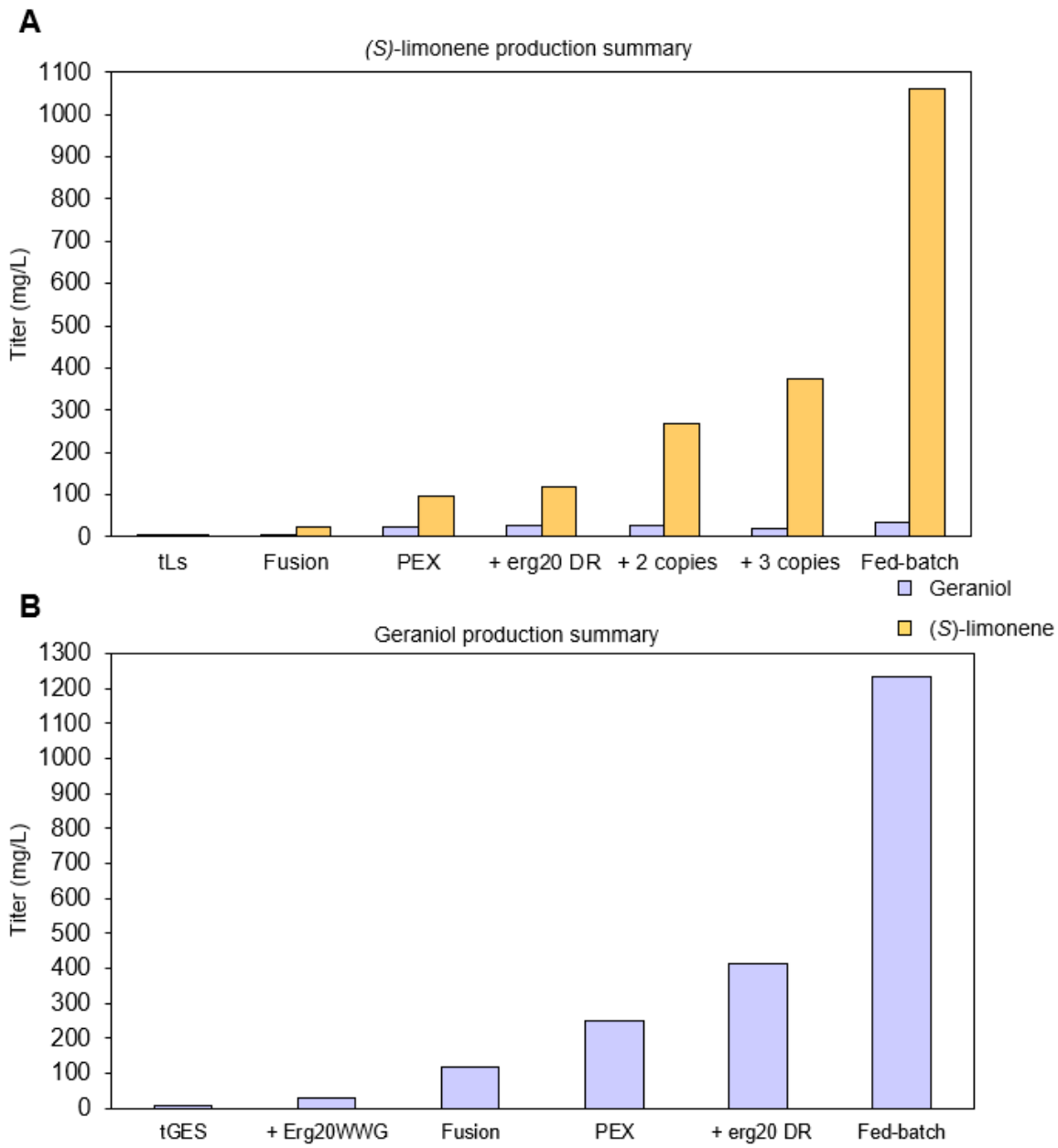

Figure S3: Strategies summary of monoterpenoid production in this study. **A.** (*S*)-limonene production. **B.** Geraniol production.

References

[1] M. Avalos, P. Garbeva, L. Vader, G. P. van Wezel, J. S. Dickschat, and D. Ulanova, "Biosynthesis, evolution and ecology of microbial terpenoids," *Natural Product Reports*, vol. 39, no. 2, pp. 249–272, 2022, doi: 10.1039/D1NP00047K.

[2] M. Rodríguez-Concepción, "Plant Isoprenoids: A General Overview," in *Plant Isoprenoids: Methods and Protocols*, M. Rodríguez-Concepción, Ed., in Methods in Molecular Biology. New York, NY: Springer, 2014, pp. 1–5. doi: 10.1007/978-1-4939-0606-2_1.

[3] "CHEMnetBASE, Dictionnary of natural products." https://dnp.chemnetbase.com/chemical/ChemicalSearch.xhtml?dswid=5324

[4] S. D. Tetali, "Terpenes and isoprenoids: a wealth of compounds for global use," *Planta*, vol. 249, no. 1, pp. 1–8, Jan. 2019, doi: 10.1007/s00425-018-3056-x.

[5] K. W. George, J. Alonso-Gutierrez, J. D. Keasling, and T. S. Lee, "Isoprenoid Drugs, Biofuels, and Chemicals—Artemisinin, Farnesene, and Beyond," in *Biotechnology of Isoprenoids*, J. Schrader and J. Bohlmann, Eds., in Advances in Biochemical Engineering/Biotechnology. Cham: Springer International Publishing, 2015, pp. 355–389. doi: 10.1007/10_2014_288.

[6] V. J. J. Martin, D. J. Pitera, S. T. Withers, J. D. Newman, and J. D. Keasling, "Engineering a mevalonate pathway in Escherichia coli for production of terpenoids," *Nat Biotechnol*, vol. 21, no. 7, Art. no. 7, Jul. 2003, doi: 10.1038/nbt833.

[7] W. Yang, X. Chen, Y. Li, S. Guo, Z. Wang, and X. Yu, "Advances in Pharmacological Activities of Terpenoids," *Natural Product Communications*, vol. 15, no. 3, p. 1934578X20903555, Mar. 2020, doi: 10.1177/1934578X20903555.

[8] U. Bathe and A. Tissier, "Cytochrome P450 enzymes: A driving force of plant diterpene diversity," *Phytochemistry*, vol. 161, pp. 149–162, May 2019, doi: 10.1016/j.phytochem.2018.12.003.

[9] M. C. F. de L. Veiga Larissa Sousa da Silva, Larissa Silveira Moreira Wiedemann, Valdir F. da, "A Brief History of Terpenoids," in *Terpenoids Against Human Diseases*, CRC Press, 2019.

[10] E. Pichersky and R. A. Raguso, "Why do plants produce so many terpenoid compounds?," *New Phytologist*, vol. 220, no. 3, pp. 692–702, 2018, doi: 10.1111/nph.14178.

[11] K. C. Nicolaou *et al.*, "Total Synthesis of Eleutherobin," *Angewandte Chemie International Edition in English*, vol. 36, no. 22, pp. 2520–2524, 1997, doi: 10.1002/anie.199725201.

[12] E. Fordjour *et al.*, "Toward improved terpenoids biosynthesis: strategies to enhance the capabilities of cell factories," *Bioresources and Bioprocessing*, vol. 9, no. 1, p. 6, Jan. 2022, doi: 10.1186/s40643-022-00493-8.

[13] C. J. Paddon *et al.*, "High-level semi-synthetic production of the potent antimalarial artemisinin," *Nature*, vol. 496, no. 7446, Art. no. 7446, Apr. 2013, doi: 10.1038/nature12051.

[14] J. Zhang *et al.*, "A microbial supply chain for production of the anti-cancer drug vinblastine," *Nature*, vol. 609, no. 7926, Art. no. 7926, Sep. 2022, doi: 10.1038/s41586-022-05157-3.

[15] M. Yang, N. R. Baral, B. A. Simmons, J. C. Mortimer, P. M. Shih, and C. D. Scown, "Accumulation of high-value bioproducts in planta can improve the economics of advanced biofuels," *Proceedings of the National Academy of Sciences*, vol. 117, no. 15, pp. 8639–8648, Apr. 2020, doi: 10.1073/pnas.2000053117.

[16] Y. Ren, S. Liu, G. Jin, X. Yang, and Y. J. Zhou, “Microbial production of limonene and its derivatives: Achievements and perspectives,” *Biotechnology Advances*, vol. 44, p. 107628, Nov. 2020, doi: 10.1016/j.biotechadv.2020.107628.
[17] T. C. Chen, C. O. D. Fonseca, and A. H. Schönthal, “Preclinical development and clinical use of perillyl alcohol for chemoprevention and cancer therapy,” *Am J Cancer Res*, vol. 5, no. 5, pp. 1580–1593, Apr. 2015.
[18] K. Sebei, F. Sakouhi, W. Herchi, M. L. Khouja, and S. Boukhchina, “Chemical composition and antibacterial activities of seven Eucalyptus species essential oils leaves,” *Biol Res*, vol. 48, no. 1, p. 7, Jan. 2015, doi: 10.1186/0717-6287-48-7.
[19] “Geraniol induces cooperative interaction of apoptosis and autophagy to elicit cell death in PC-3 prostate cancer cells.” https://www.spandidos-publications.com/ijo/40/5/1683 (accessed May 21, 2023).
[20] Y. Liu, X. Ma, H. Liang, G. Stephanopoulos, and K. Zhou, “Monoterpenoid biosynthesis by engineered microbes,” *Journal of Industrial Microbiology and Biotechnology*, vol. 48, no. 9–10, p. kuab065, Dec. 2021, doi: 10.1093/jimb/kuab065.
[21] F. J. Scariot, M. S. Pansera, A. P. Longaray Delamare, and S. Echeverrigaray, “Antifungal activity of monoterpenes against the model yeast Saccharomyces cerevisiae,” *Journal of Food Processing and Preservation*, vol. 45, no. 5, p. e15433, 2021, doi: 10.1111/jfpp.15433.
[22] T. C. R. Brennan, C. D. Turner, J. O. Krömer, and L. K. Nielsen, “Alleviating monoterpene toxicity using a two-phase extractive fermentation for the bioproduction of jet fuel mixtures in Saccharomyces cerevisiae,” *Biotechnology and Bioengineering*, vol. 109, no. 10, pp. 2513–2522, 2012, doi: 10.1002/bit.24536.
[23] D. Mendez-Perez *et al.*, “Production of jet fuel precursor monoterpenoids from engineered Escherichia coli,” *Biotechnology and Bioengineering*, vol. 114, no. 8, pp. 1703–1712, 2017, doi: 10.1002/bit.26296.
[24] M. J. C. Fischer, S. Meyer, P. Claudel, M. Bergdoll, and F. Karst, “Metabolic engineering of monoterpene synthesis in yeast,” *Biotechnology and Bioengineering*, vol. 108, no. 8, pp. 1883–1892, 2011, doi: 10.1002/bit.23129.
[25] C. Ignea, M. Pontini, M. E. Maffei, A. M. Makris, and S. C. Kampranis, “Engineering Monoterpene Production in Yeast Using a Synthetic Dominant Negative Geranyl Diphosphate Synthase,” *ACS Synth. Biol.*, vol. 3, no. 5, pp. 298–306, May 2014, doi: 10.1021/sb400115e.
[26] Z. Wang *et al.*, “Recent advances in the biosynthesis of isoprenoids in engineered Saccharomyces cerevisiae,” in *Advances in Applied Microbiology*, G. M. Gadd and S. Sariaslani, Eds., Academic Press, 2021, pp. 1–35. doi: 10.1016/bs.aambs.2020.11.001.
[27] K.-K. Hong and J. Nielsen, “Metabolic engineering of Saccharomyces cerevisiae: a key cell factory platform for future biorefineries,” *Cell. Mol. Life Sci.*, vol. 69, no. 16, pp. 2671–2690, Aug. 2012, doi: 10.1007/s00018-012-0945-1.
[28] J. Nielsen and J. D. Keasling, “Engineering Cellular Metabolism,” *Cell*, vol. 164, no. 6, pp. 1185–1197, Mar. 2016, doi: 10.1016/j.cell.2016.02.004.
[29] L. Jiang, L. Huang, J. Cai, Z. Xu, and J. Lian, “Functional expression of eukaryotic cytochrome P450s in yeast,” *Biotechnology and Bioengineering*, vol. 118, no. 3, pp. 1050–1065, 2021, doi: 10.1002/bit.27630.
[30] J. Liu, W. Zhang, G. Du, J. Chen, and J. Zhou, “Overproduction of geraniol by enhanced precursor supply in Saccharomyces cerevisiae,” *Journal of Biotechnology*, vol. 168, no. 4, pp. 446–451, Dec. 2013, doi: 10.1016/j.jbiotec.2013.10.017.
[31] J. Zhao, X. Bao, C. Li, Y. Shen, and J. Hou, “Improving monoterpene geraniol production through geranyl diphosphate synthesis regulation in Saccharomyces cerevisiae,”

Appl Microbiol Biotechnol, vol. 100, no. 10, pp. 4561–4571, May 2016, doi: 10.1007/s00253-016-7375-1.

[32] J. Zhao, C. Li, Y. Zhang, Y. Shen, J. Hou, and X. Bao, "Dynamic control of ERG20 expression combined with minimized endogenous downstream metabolism contributes to the improvement of geraniol production in Saccharomyces cerevisiae," *Microbial Cell Factories*, vol. 16, no. 1, p. 17, Jan. 2017, doi: 10.1186/s12934-017-0641-9.

[33] B. Peng, L. K. Nielsen, S. C. Kampranis, and C. E. Vickers, "Engineered protein degradation of farnesyl pyrophosphate synthase is an effective regulatory mechanism to increase monoterpene production in Saccharomyces cerevisiae," *Metabolic Engineering*, vol. 47, pp. 83–93, May 2018, doi: 10.1016/j.ymben.2018.02.005.

[34] S. Cheng *et al.*, "Orthogonal Engineering of Biosynthetic Pathway for Efficient Production of Limonene in Saccharomyces cerevisiae," *ACS Synth. Biol.*, vol. 8, no. 5, pp. 968–975, May 2019, doi: 10.1021/acssynbio.9b00135.

[35] S. Dusséaux, W. T. Wajn, Y. Liu, C. Ignea, and S. C. Kampranis, "Transforming yeast peroxisomes into microfactories for the efficient production of high-value isoprenoids," *Proc. Natl. Acad. Sci. U.S.A.*, vol. 117, no. 50, pp. 31789–31799, Dec. 2020, doi: 10.1073/pnas.2013968117.

[36] X. Chen, J. Zaro, and W.-C. Shen, "Fusion Protein Linkers: Property, Design and Functionality," *Adv Drug Deliv Rev*, vol. 65, no. 10, pp. 1357–1369, Oct. 2013, doi: 10.1016/j.addr.2012.09.039.

[37] G. Scalcinati *et al.*, "Dynamic control of gene expression in Saccharomyces cerevisiae engineered for the production of plant sesquitepene α-santalene in a fed-batch mode," *Metabolic Engineering*, vol. 14, no. 2, pp. 91–103, Mar. 2012, doi: 10.1016/j.ymben.2012.01.007.

[38] K. Paramasivan and S. Mutturi, "Progress in terpene synthesis strategies through engineering of Saccharomyces cerevisiae," *Critical Reviews in Biotechnology*, vol. 37, no. 8, pp. 974–989, Nov. 2017, doi: 10.1080/07388551.2017.1299679.

[39] W. Xie, L. Ye, X. Lv, H. Xu, and H. Yu, "Sequential control of biosynthetic pathways for balanced utilization of metabolic intermediates in Saccharomyces cerevisiae," *Metabolic Engineering*, vol. 28, pp. 8–18, Mar. 2015, doi: 10.1016/j.ymben.2014.11.007.

[40] J. Alonso-Gutierrez *et al.*, "Metabolic engineering of Escherichia coli for limonene and perillyl alcohol production," *Metabolic Engineering*, vol. 19, pp. 33–41, Sep. 2013, doi: 10.1016/j.ymben.2013.05.004.

[41] X. Zhang, X. Liu, Y. Meng, L. Zhang, J. Qiao, and G.-R. Zhao, "Combinatorial engineering of Saccharomyces cerevisiae for improving limonene production," *Biochemical Engineering Journal*, vol. 176, p. 108155, Dec. 2021, doi: 10.1016/j.bej.2021.108155.

[42] T. Li *et al.*, "Metabolic Engineering of Saccharomyces cerevisiae To Overproduce Squalene," *J. Agric. Food Chem.*, vol. 68, no. 7, pp. 2132–2138, Feb. 2020, doi: 10.1021/acs.jafc.9b07419.

[43] J. Li *et al.*, "Simultaneous Improvement of Limonene Production and Tolerance in Yarrowia lipolytica through Tolerance Engineering and Evolutionary Engineering," *ACS Synth. Biol.*, vol. 10, no. 4, pp. 884–896, Apr. 2021, doi: 10.1021/acssynbio.1c00052.

[44] T. P. Korman, P. H. Opgenorth, and J. U. Bowie, "A synthetic biochemistry platform for cell free production of monoterpenes from glucose," *Nat Commun*, vol. 8, no. 1, Art. no. 1, May 2017, doi: 10.1038/ncomms15526.

[45] L. Kvittingen, B. J. Sjursnes, and R. Schmid, "Limonene in Citrus: A String of Unchecked Literature Citings?," *J. Chem. Educ.*, vol. 98, no. 11, pp. 3600–3607, Nov. 2021, doi: 10.1021/acs.jchemed.1c00363.

[46] A. O. Durço, L. S. R. Conceição, D. S. De Souza, C. A. Lima, J. D. S. S. Quintans, and M. R. Viana Dos Santos, “Perillyl alcohol as a treatment for cancer: A systematic review,” *Phytomedicine Plus*, vol. 1, no. 3, p. 100090, Aug. 2021, doi: 10.1016/j.phyplu.2021.100090.
[47] T. C. Chen, C. O. da Fonseca, D. Levin, and A. H. Schönthal, “The Monoterpenoid Perillyl Alcohol: Anticancer Agent and Medium to Overcome Biological Barriers,” *Pharmaceutics*, vol. 13, no. 12, p. 2167, Dec. 2021, doi: 10.3390/pharmaceutics13122167.
[48] E. Jongedijk *et al.*, “Novel routes towards bioplastics from plants: elucidation of the methylperillate biosynthesis pathway from Salvia dorisiana trichomes,” *Journal of Experimental Botany*, vol. 71, no. 10, pp. 3052–3065, May 2020, doi: 10.1093/jxb/eraa086.
[49] K.-D. Entian and P. Kötter, “23 Yeast Mutant and Plasmid Collections,” in *Methods in Microbiology*, A. J. P. Brown and M. Tuite, Eds., in Yeast Gene Analysis, vol. 26. Academic Press, 1998, pp. 431–449. doi: 10.1016/S0580-9517(08)70344-1.
[50] S. Kim and J.-S. Hahn, “Efficient production of 2,3-butanediol in Saccharomyces cerevisiae by eliminating ethanol and glycerol production and redox rebalancing,” *Metabolic Engineering*, vol. 31, pp. 94–101, Sep. 2015, doi: 10.1016/j.ymben.2015.07.006.
[51] Amberg DC, Burke DJ, Strathern JN, “Methods in Yeast Genetics: A Cold Spring Harbor Laboratory Course Manual. 2005 Edition,” 2005.
[52] M. Lõoke, K. Kristjuhan, and A. Kristjuhan, “EXTRACTION OF GENOMIC DNA FROM YEASTS FOR PCR-BASED APPLICATIONS,” *Biotechniques*, vol. 50, no. 5, pp. 325–328, May 2011, doi: 10.2144/000113672.
[53] R. D. Gietz and R. H. Schiestl, “Large-scale high-efficiency yeast transformation using the LiAc/SS carrier DNA/PEG method,” *Nat Protoc*, vol. 2, no. 1, Art. no. 1, Jan. 2007, doi: 10.1038/nprot.2007.15.
[54] J. Hong, S.-H. Park, S. Kim, S.-W. Kim, and J.-S. Hahn, “Efficient production of lycopene in Saccharomyces cerevisiae by enzyme engineering and increasing membrane flexibility and NAPDH production,” *Appl Microbiol Biotechnol*, vol. 103, no. 1, pp. 211–223, Jan. 2019, doi: 10.1007/s00253-018-9449-8.
[55] K. Labun, T. G. Montague, M. Krause, Y. N. Torres Cleuren, H. Tjeldnes, and E. Valen, “CHOPCHOP v3: expanding the CRISPR web toolbox beyond genome editing,” *Nucleic Acids Research*, vol. 47, no. W1, pp. W171–W174, Jul. 2019, doi: 10.1093/nar/gkz365.
[56] S. Baek, J. C. Utomo, J. Y. Lee, K. Dalal, Y. J. Yoon, and D.-K. Ro, “The yeast platform engineered for synthetic gRNA-landing pads enables multiple gene integrations by a single gRNA/Cas9 system,” *Metabolic Engineering*, vol. 64, pp. 111–121, Mar. 2021, doi: 10.1016/j.ymben.2021.01.011.
[57] S.-H. Park, K. Lee, J. W. Jang, and J.-S. Hahn, “Metabolic Engineering of Saccharomyces cerevisiae for Production of Shinorine, a Sunscreen Material, from Xylose,” *ACS Synth. Biol.*, vol. 8, no. 2, pp. 346–357, Feb. 2019, doi: 10.1021/acssynbio.8b00388.
[58] J. M. Kim, S. Vanguri, J. D. Boeke, A. Gabriel, and D. F. Voytas, “Transposable Elements and Genome Organization: A Comprehensive Survey of Retrotransposons Revealed by the Complete Saccharomyces cerevisiae Genome Sequence,” *Genome Res.*, vol. 8, no. 5, pp. 464–478, Jan. 1998, doi: 10.1101/gr.8.5.464.
[59] J. Yuan and C. B. Ching, “Combinatorial Assembly of Large Biochemical Pathways into Yeast Chromosomes for Improved Production of Value-added Compounds,” *ACS Synth. Biol.*, vol. 4, no. 1, pp. 23–31, Jan. 2015, doi: 10.1021/sb500079f.
[60] U. Gueldener, J. Heinisch, G. J. Koehler, D. Voss, and J. H. Hegemann, “A second set of loxP marker cassettes for Cre-mediated multiple gene knockouts in budding yeast,” *Nucleic Acids Research*, vol. 30, no. 6, p. e23, Mar. 2002, doi: 10.1093/nar/30.6.e23.

[61] H. Liu and J. H. Naismith, “An efficient one-step site-directed deletion, insertion, single and multiple-site plasmid mutagenesis protocol,” *BMC Biotechnology*, vol. 8, no. 1, p. 91, Dec. 2008, doi: 10.1186/1472-6750-8-91.
[62] W. C. DeLoache, Z. N. Russ, and J. E. Dueber, “Towards repurposing the yeast peroxisome for compartmentalizing heterologous metabolic pathways,” *Nat Commun*, vol. 7, no. 1, p. 11152, Mar. 2016, doi: 10.1038/ncomms11152.
[63] G.-Z. Jiang *et al.*, “Manipulation of GES and ERG20 for geraniol overproduction in Saccharomyces cerevisiae,” *Metabolic Engineering*, vol. 41, pp. 57–66, May 2017, doi: 10.1016/j.ymben.2017.03.005.
[64] E. Carsanba, M. Pintado, and C. Oliveira, “Fermentation Strategies for Production of Pharmaceutical Terpenoids in Engineered Yeast,” *Pharmaceuticals (Basel)*, vol. 14, no. 4, p. 295, Mar. 2021, doi: 10.3390/ph14040295.
[65] Z. Lu, B. Peng, B. E. Ebert, G. Dumsday, and C. E. Vickers, “Auxin-mediated protein depletion for metabolic engineering in terpene-producing yeast,” *Nat Commun*, vol. 12, no. 1, Art. no. 1, Feb. 2021, doi: 10.1038/s41467-021-21313-1.
[66] C. W. T. van Roermund *et al.*, “Identification of a Peroxisomal ATP Carrier Required for Medium-Chain Fatty Acid β-Oxidation and Normal Peroxisome Proliferation in Saccharomyces cerevisiae,” *Mol Cell Biol*, vol. 21, no. 13, pp. 4321–4329, Jul. 2001, doi: 10.1128/MCB.21.13.4321-4329.2001.
[67] Y. Chen *et al.*, “Primary and Secondary Metabolic Effects of a Key Gene Deletion (ΔYPL062W) in Metabolically Engineered Terpenoid-Producing Saccharomyces cerevisiae,” *Appl Environ Microbiol*, vol. 85, no. 7, pp. e01990-18, Mar. 2019, doi: 10.1128/AEM.01990-18.
[68] C. J. D. Mau, F. Karp, M. Ito, G. Honda, and R. B. Croteau, “A candidate cDNA clone for (−)-limonene-7-hydroxylase from Perilla frutescens,” *Phytochemistry*, vol. 71, no. 4, pp. 373–379, Mar. 2010, doi: 10.1016/j.phytochem.2009.12.002.
[69] C. Haudenschild, M. Schalk, F. Karp, and R. Croteau, “Functional Expression of Regiospecific Cytochrome P450 Limonene Hydroxylases from Mint (Mentha spp.) in Escherichia coli and Saccharomyces cerevisiae,” *Archives of Biochemistry and Biophysics*, vol. 379, no. 1, pp. 127–136, Jul. 2000, doi: 10.1006/abbi.2000.1864.
[70] S.-H. Park and J.-S. Hahn, “Development of an efficient cytosolic isobutanol production pathway in Saccharomyces cerevisiae by optimizing copy numbers and expression of the pathway genes based on the toxic effect of α-acetolactate,” *Sci Rep*, vol. 9, p. 3996, Mar. 2019, doi: 10.1038/s41598-019-40631-5.
[71] A. J. Simkin *et al.*, “Characterization of the plastidial geraniol synthase from Madagascar periwinkle which initiates the monoterpenoid branch of the alkaloid pathway in internal phloem associated parenchyma,” *Phytochemistry*, vol. 85, pp. 36–43, Jan. 2013, doi: 10.1016/j.phytochem.2012.09.014.
[72] S. M. Colby, W. R. Alonso, E. J. Katahira, D. J. McGarvey, and R. Croteau, “4S-limonene synthase from the oil glands of spearmint (Mentha spicata). cDNA isolation, characterization, and bacterial expression of the catalytically active monoterpene cyclase.,” *Journal of Biological Chemistry*, vol. 268, no. 31, pp. 23016–23024, Nov. 1993, doi: 10.1016/S0021-9258(19)49419-2.